Theme C1: General aspects

Measurement of Service Stress and Fatigue Life Evaluation of Bridges

Mesure des contraintes à l'état de service et évaluation de la durée de vie des ponts

Betriebsspannungsmessungen und Lebensdauerberechnungen von Brücken

Kentaro YAMADA
Professor
Nagoya University
Nagoya, Japan

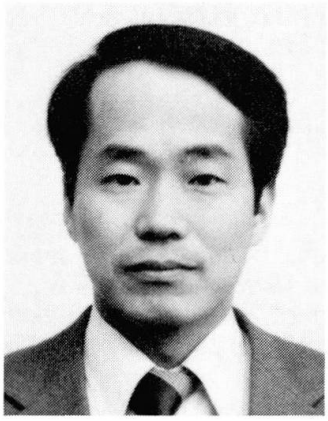

Kentaro Yamada, born 1946, received his civil engineering degree at Nagoya University, and PhD at University of Maryland, MD, USA. Since then, he has been involved in fatigue tests of welded structures, application of fracture mechanics, and field measurement of service stresses of highway bridges.

SUMMARY

Service stresses have been measured by using a histogram recorder. Fatigue life is evaluated using the Miner's cumulative damage rule and the ECCS fatigue-strength diagrams. Calculated fatigue lives of main members are longer than a hundred years whereas for secondary members, relatively short. These results are consistent with the observation of major fatigue cracks in secondary members.

RÉSUMÉ

Les contraintes à l'état de service ont été mesurées à l'aide d'un enregistreur d'histogramme. La durée de vie est évaluée en utilisant la loi de cumul du dommage de Miner et les courbes de résistance à la fatigue du CECM. Les durées de vie calculées pour les éléments principaux sont supérieures à cent ans, alors que celles des éléments secondaires sont relativement courtes. Ces résultats sont en accord avec les observations des principales fissures de fatigue recensées dans les éléments secondaires.

ZUSAMMENFASSUNG

Mit einem Histogramm-Registriergerät wurden Betriebsspannungen gemessen. Für die Berechnung der Lebensdauer werden das Gesetz von Miner über die Schadensakkumulation und die EKS-Ermüdungsfestigkeitskurven verwendet. Die so berechnete Lebenserwartung beträgt für die Haupttragelemente mehr als hundert Jahre, während sie für die untergeordneten Elemente relativ gering ausfällt. Diese Resultate stimmen mit der Beobachtung überein, dass die grössten Ermüdungsrisse in untergeordneten Elementen auftreten.

1. INTRODUCTION

Both stresses and their frequency of in the structural members of highway bridges have increased due to an increasing weight and number of trucks in the past two decades in Japan. It has led to some fatigue cracks in structural members in highway bridges [2,3]. Although the cracks were mainly found in the secondary members and caused no immediate danger to the bridge, they may grow in size with stress cycles and cause serious maintenance problems to the bridges. In order to investigate the cause of cracks, stress measurements were often carried out.

This study was to evaluate the fatigue life of structural members in five steel bridges based on the measured stress range histograms. The bridges include a riveted truss bridge, a composite plate girder bridge, a non-composite plate girder bridge, a box girder bridge with orthotropic steel deck and an arch bridge subjected to different traffic conditions.

2. SERVICE STRESS MEASUREMENT OF BRIDGES

2.1 Description of Bridges

1) Bridge A: It is a 60-year old riveted Warren truss bridge, as shown in Fig. 1, with a span of 73 m and a 16 m wide roadway. The bridge is daily subjected to about 250 trains at a speed of about 10 km/h and about 10,000 vehicles, in which 11 percent are trucks. The traffic is considered rather light in Japan.

2) Bridge B: It is a welded plate girder bridge built in 1967, with a span of 27.9 m and a 7.0 m wide roadway for two lanes, as shown in Fig.2. The spacings of main girders are 2.0 m and the sway bracings are placed at 5.58 m intervals. The reinforced concrete deck was originally 23 cm thick, and was later added by a 12 cm thick steel-fiber reinforced concrete in 1979. It is a private bridge in a steel works. Although about twenty special trucks of more than 785 kN (80 tons) pass on it daily, the number of daily truck traffic is very small.

3) Bridge C: It is a two-span continuous plate girder bridge built in 1964, with eight main girders spaced at 3.2 m intervals, as shown in Fig.3. The total length is 40 m with two spans of 20 m each. The roadway is for six lanes, threc lanes for each direction. The deck is made of 19 cm thick reinforced concrete slab. The bridge situates in an industrial area and carries about 100,000 vehicles daily. About half of the passing vehicles are trucks and it is considered to be under severe traffic condition. The bridge was repaired and retrofitted in 1982, when cracks were found in the fillet weld at the upper end of vertical stiffener. The stress measurement was carried out in 1984 [4].

4) Bridge D: It is a three-span box girder bridge with orthotropic steel decks, built in 1964. It has a 96 m center span and two 77 m side spans, as shown in Fig.4. It is situated on the same route as Bridge C, and is also subjected to severe traffic condition. Several fatigue cracks were found in the corner of diaphragms, and rehabilitation works were carried out in 1989.

5) Bridge E: It is a two-hinge deck type arch bridge built in 1964. The arch has 54 m span and the width of roadway is 9.9 m, as shown in Fig.5. The bridge is subjected to about 80,000 vehicles every day, and 26 percent of them are trucks. The bridge is also subjected to severe traffic condition. Fatigue cracks were found in stringers of floor system and vertical members of arch. The cracks of the stringers were repaired and the cracked parts were stiffened. Further repair and strengthening of the arch and replacement of concrete slab into orthotropic steel deck are underway.

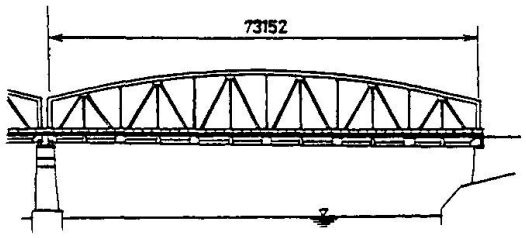

Fig.1 Bridge A: Riveted truss bridge

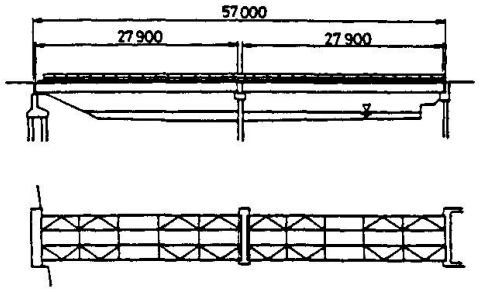

Fig.2 Bridge B: Composite plate girder bridge

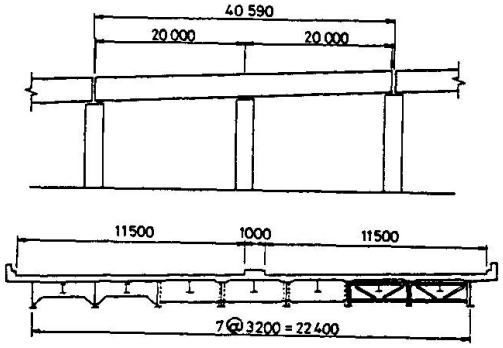

Fig.3 Bridge C: Non-composite plate girder bridge

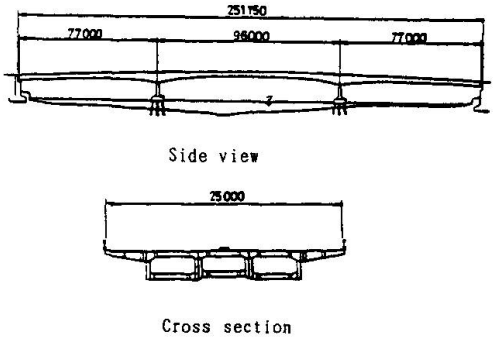

Fig.4 Bridge D: Three span continuous box girder bridge

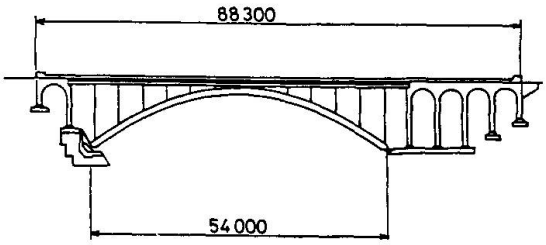

Fig.5 Bridge E: Deck type arch bridge

2.2 Measurement under Model Vehicle of Controlled Weight

Trucks of controlled weight of 196 kN (20 tons) are often chosen to be model vehicles in order to represent the design truck T-20. The model vehicles are placed at several points on the bridge or driven at a certain speed through the bridge. Static and dynamic strains are measured by using strain gages. The dynamic strains are recorded in magnetic tape data recorder, and then monitored by a synchroscope or a pen-recorder. The test results are often compared with the analytical results. This type of measurements causes some difficulties as to stop the normal traffics, which are often very heavy in Japan.

2.3 Measurement of Service Stress Range Histogram

Stresses under service condition are important to evaluate the durability of structures. Service stresses can be measured by using a Histogram Recorder, as

shown in Fig.6 [9]. It analyzes the strain waves in real time and records the stress ranges and the number of their occurrence. The analysis may be based on rainflow counting method, peak counting method, level crossing counting method, and so on. The rainflow counting method was used in this study to obtain stress range histogram. The Histogram Recorder has some advantages as that it requires no traffic control, and the disadvantage is that it distinguishes neither the type of trucks nor their axle weight. Therefore, stresses under model vehicle with controlled weight are often measured and used as reference values.

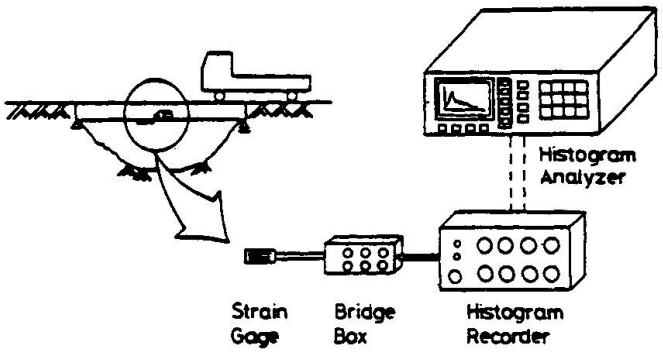

Fig.6 Measurement of stress histogram

Examples of the stress range histogram measured for 24 hours are shown in Fig. 7, where the ordinate indicates stress range and the abscissa shows the number of half stress cycles in logarithmic scale. The stress ranges corresponding to the model vehicles are also shown as reference values.

The stress histogram of a diagonal member of the Bridge A is shown in Fig.7a. The model vehicles are a 22.5-ton dump truck with 3 axles and a train with 6 cars. It seems that the upper peak of stress cycles is caused by the trains. The stress cycles below the reference value by the model truck may be caused by lighter trucks and the other vehicles and that above the reference value by the train is considered to be caused when the trucks and the train passed on the bridge simultaneously.

Figs.7b and 7c show stress range histograms measured at a lower flange and the upper end of a vertical stiffener of Bridge B, respectively. The measured maximum stress range in the lower flange is close to reference stress range by the 1140 kN (116 tons) trailer truck. And that in the lower flange of Bridge B is about 80 MPa, about twice of that in the diagonal members of Bridge A.

Fig.7d shows stress range histogram measured at bottom of longitudinal rib in the orthotropic steel deck of Bridge D. The model vehicle was a crane truck of 364 kN (37.1 tons). The maximum stress range was about 105 MPa, about twice of stresses due to the model vehicle. It is either because the trucks weigh more than the model vehicle, or because heavy trucks crossed the bridge simultaneously. There was extremely large number of low stress ranges. This may be explained by the frequent passage of small trucks or vibration in the orthotropic steel deck due to the passing traffics.

Fig.7e shows stress range histogram measured at the arch rib of passing lane side of Bridge E. The reference stress ranges due to a truck of 206 kN (21 tons) passing on the slow lane or on the passing lane, or three same trucks are also shown in the figure. The measured stress range were larger than the stresses by the three trucks. It implies that vehicles weighed more than the model trucks frequently passed on the bridge.

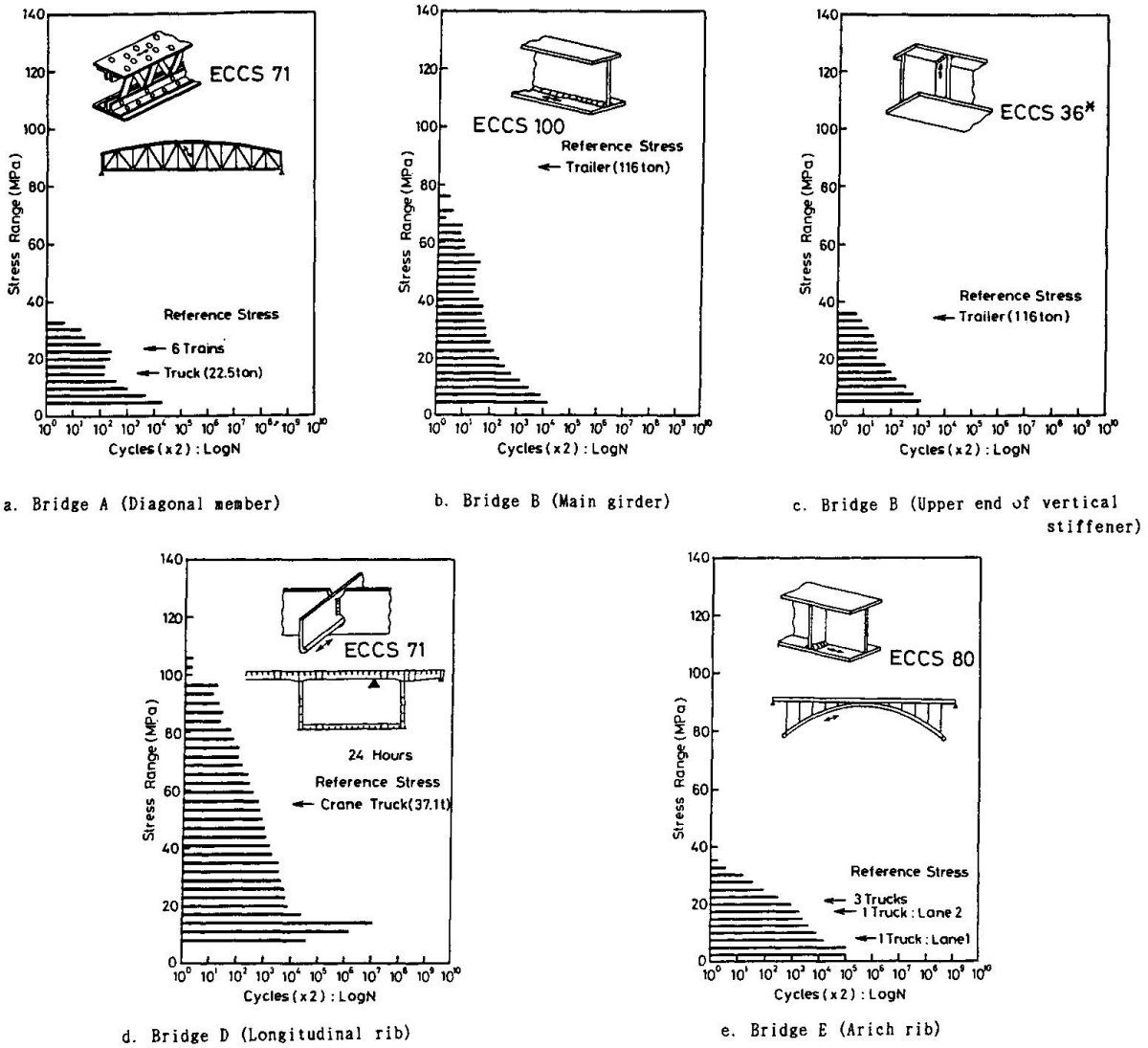

Fig.7 Example of stress range histogram records

The stress range histograms of Bridges D and E were different from that of Bridges A and B. This is because the volume of traffics is much greater in Bridges D and E than in Bridges A and B. For example, about 250 trains and 10,000 vehicles passed on Bridge A, while over 100,000 vehicles passed on Bridge D and about 80,000 vehicles passed on Bridge E for 24 hours.

3. EVALUATION OF FATIGUE LIFE BASED ON MEASURED STRESS RANGE HISTOGRAM

3.1 Detail Categories

In this study the design S-N diagrams specified in the ECCS Recommendation for the Fatigue Design of Steel Structures [8] were used to evaluate the fatigue strength of weld details. Since the design S-N diagrams correspond to the mean-2xs (s:standard deviation) S-N diagrams, the computed fatigue life is the lower bound fatigue life. The design S-N diagrams are given for classified structural detail. The detail categories evaluated for fatigue life in this study are also shown in Fig.7.

1) Bridge A: Riveted joints are classified as ECCS 71.

2) Bridge B and C: The lower flange of the plate girder is fillet-welded to the web, and this detail is classified as ECCS 100. The upper end of the vertical stiffener (connection plate) with a cross beam or a lateral bracing can be considered as load-carrying fillet weld, and it is ECCS 36 if root-cracking is assumed.

3) Bridge D: The stress range of longitudinal ribs welded to lateral ribs in the orthotropic steel deck is used from that measured at the bottom of the longitudinal rib. The welds are assumed as load-carrying fillet weld and it is classified as ECCS 71 for toe crack.

4) Bridge E: The upper and the lower ends of the vertical members are fillet-welded to splice plates, which are then riveted to the arch rib and the floor system. The weld detail is classified as ECCS 71. The arch rib has stiffeners that are fillet-welded to the arch rib web. The detail is non-load-carrying fillet weld, and is classified as ECCS 80.

3.2 Evaluation of Fatigue Life Based on Service Loading

Two types of design S-N diagrams specified in the ECCS Recommendation are used to evaluate the fatigue damage based on the stress range histogram, as shown in Fig.8.

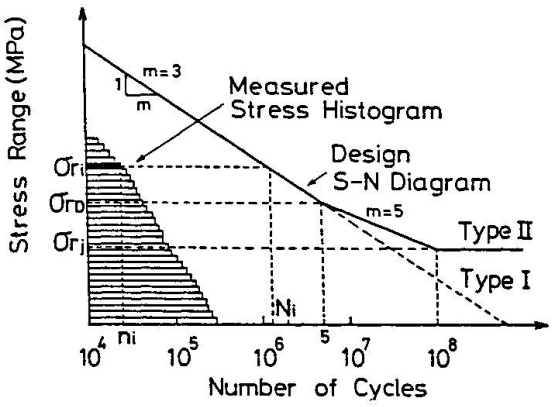

Fig.8 ECCS design S-N diagram

1) Type I (Modified miner's rule): The S-N diagram of slope of m=3 is extended linearly.
2) Type II (Three line method): The slope of the S-N diagram m is equal to 3 for N less than 5 million cycles, and 5 for N between 5 million and 100 million cycles. Stress ranges below the cut-off limit are neglected.

To carry out the damage calculation, the actual number of stress cycles n_i corresponding to each stress range σ_{ri} is obtained first from the histogram. Then the number of cycles to failure N_i corresponding to each σ_{ri} is obtained from the S-N diagram. The fatigue damage D is the sum of n_i/N_i for all stress range in the histogram, i.e.,

$$D = \Sigma\ (n_i/N_i) \qquad (1)$$

where it is assumed that the detail fails due to fatigue, when D becomes unity. Since all the measured stress range histograms in this study are for 24 hours, the

evaluated D according to Eq.1 indicates the fatigue damage in one day. Assuming that the data is obtained in a typical day and that the traffic condition will remain unchanged, the expected fatigue life L is given by the following equation.

$$L(\text{year}) = 1/(365 \times D) \qquad (2)$$

The fatigue life may also be evaluated by using the equivalent stress range concept. The equivalent stress range $\sigma_{r,eq}$ is obtained from the S-N diagrams by assuming that the sum of n_i/N_i becomes unity at the time of fatigue failure. When one wants to use the type II S-N diagram (three line method), those stress range below the fatigue limit are considered by using slope m = 5 and those below the cut-off limit are neglected in the calculation of $\sigma_{r,eq}$ [8].

4. FATIGUE EVALUATION AND DISCUSSION

4.1 Influence of Traffic

Fatigue lives of the above-mentioned structural details in the Bridges A and B computed from the measured stress histograms are plotted in Fig.9. The two bridges were subjected to relatively light traffics, and their fatigue life are shown by the solid symbols in Fig.9. The fatigue life of the main members of Bridge A yields to more than 220 years, and that of the tension flanges of Bridge B are between 120 and 140 years. Even the upper end of vertical stiffeners of Bridge B showed the life longer than 90 years. Considering that the evaluated fatigue life is the lower bound because of the use of the lower bound S-N diagrams, it may be safe to concluded that fatigue cracks would hardly occur in these details, provided that traffic condition will remain unchanged and structural deterioration such as corrosion will not take place.

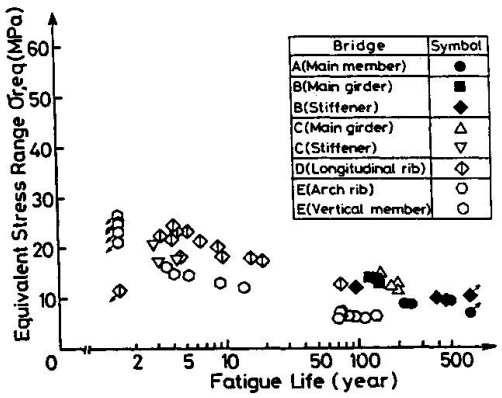

Fig.9 Equivalent stress range and fatigue life for Bridges A and B

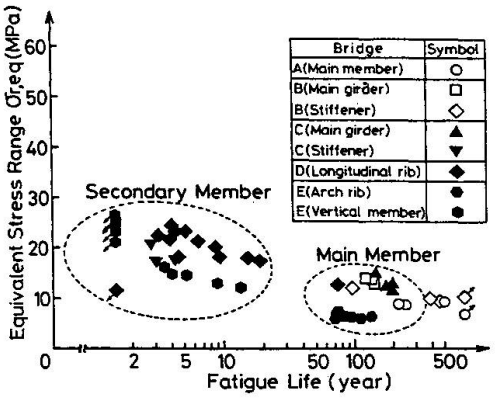

Fig.10 Equivalent stress range and fatigue life for Bridges C, D and E

Bridges C, D and E were subjected to severe traffic condition, and their fatigue lives are plotted by the solid symbols in Fig.10. If the structural details are grouped into main members and secondary members, the computed fatigue lives can be also grouped accordingly. For example, the fatigue lives of the tension flange of Bridge C are more than 100 years, and that of the arch ribs of Bridge E is between 70 and 130 years. On the contrary, the fatigue lives of the vertical members of the arch are less than 4 years, that of the longitudinal ribs in Bridge D are less than 20 years, and that of the upper and lower ends of the vertical members of Bridge E are below 15 years. Actually, the welded details in these secondary members were found susceptible to fatigue cracking previously [2,3,4]. Therefore, the fatigue lives obtained from the measured stress range histogram are a good

indicator of the severeness of structural detail against fatigue, even though the fatigue lives computed here are still inaccurate due to many uncertainties involved in the analysis.

Bridges B and C are both plate girder bridges with similar structural details, and their fatigue lives are plotted by the solid symbols in Fig. 11. It is noted that the main girder of Bridge B showed shorter fatigue life than Bridge C, although Bridge C are subjected to about 100,000 vehicles daily. This may be because Bridge B carries special vehicles of of over 785 kN (80 tons). However, the upper ends of the vertical stiffeners in Bridge B showed long fatigue lives. This may be due to the 35 cm thick concrete slab and the 2.0 m girder spacing in Bridge B. They reduced the stresses and hence increased the fatigue life. On the contrary the Bridge C has a 19 cm thick concrete slab and 3.2 m girder spacings.

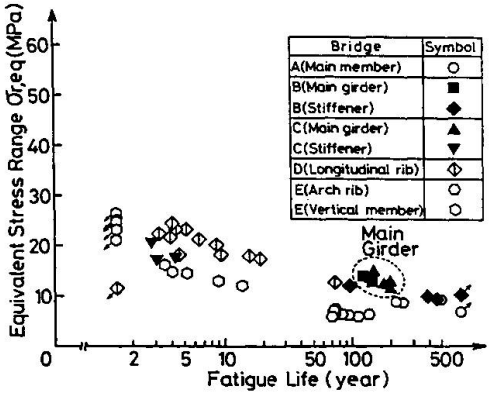

Fig.11 Equivalent stress range and fatigue life for Bridges B and C

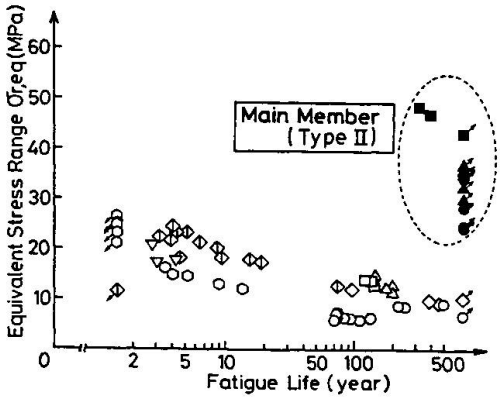

Fig.12 Equivalent stress range and fatigue damage for main members

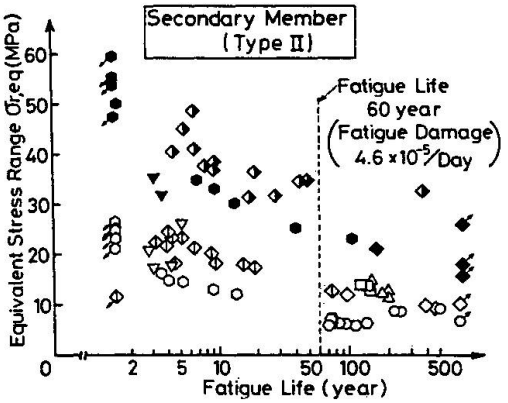

Fig.13 Equivalent stress range and fatigue damage for secondary members

4.2 Influence of S-N Diagrams

The type II S-N diagram (Three line method) was also used to evaluate the fatigue life of each detail, and the results are plotted in Figs. 12 and 13. In Fig. 12, computed fatigue life of the main members (the tension flanges and the arch ribs) using the type II S-N diagram are shown by the solid symbols. They are over 300 years, longer than that evaluated by using the type I S-N diagram. This is because most of the stress ranges in the histograms are below the cut-off limit and they are neglected in the type II S-N diagram. In the case of the arch ribs of the

bridge E, the fatigue life becomes infinite because all stress ranges are below the cut-off limit.

The fatigue lives of the secondary members are shown by the solid symbols in Fig.13. Although the equivalent stress ranges increase, the computed fatigue lives are similar to the lives computed based on the type I S-N diagram. A good part of the stress ranges in the histogram were above cut-off limit and contributed to the fatigue damages of the secondary members. Some secondary members actually experienced fatigue crackings, and therefore this trend can also be used to evaluate the severeness of stresses against fatigue.

The fatigue lives computed here should still be considered as relative values. This is because the fatigue strength in the long life region in the S-N diagrams has not yet been clarified due to the lack of experimental data. The fatigue behavior of structural details in long life region, especially under variable amplitude stress cycles, should be further investigated.

4.3 Fatigue Damage Threshold

We may be able to define fatigue damage threshold for bridge members. The fatigue damage threshold is the damage D_{th}, above which the fatigue cracking may occur in a certain period of time. As mentioned above, the fatigue prone details, known from the past experiences, showed relatively large fatigue damage, and hence yielded to short fatigue lives. The dotted line in Fig.13 clearly separate the fatigue-prone secondary members from the main members. It corresponds to fatigue life of 60 years, or daily fatigue damage of 4.6×10^{-6}.

5. SUMMARY

The measurement of the service stress ranges is important to evaluate the durability of bridges or similar steel structures against fatigue. In this study, stress histograms were collected for five bridges and evaluated. Then the fatigue damages and fatigue lives of the details were computed according to evaluated the design S-N diagrams recommended by the ECCS. The following summarizes the results.

1) The histogram of service stress ranges may be conveniently measured by a Histogram Recorder.

2) The service stress ranges often showed larger stress ranges than the stresses caused by design trucks, such as T-20 and TT-43.

3) Little possibility of fatigue cracking of the main members of highway bridges exists during service period, because the evaluated fatigue lives were in the order of a hundred years or over.

4) The fatigue lives of the secondary members, which experienced fatigue cracking previously, were much shorter than that of the main members.

5) The selection of design S-N diagrams may yield to large discrepancy in the computed fatigue life based on the service stress range histogram. Thus, it is necessary to establish better design S-N diagram in the long life region based on experimental data.

6) The evaluated fatigue life may not be as accurate as expected, but it has relative meaning in expressing the severeness of stresses in the details against fatigue.

7) The daily fatigue damage of $D = 4.6 \times 10^{-6}$ may be used as a fatigue damage threshold value to identify whether the detail is fatigue-prone or not in highway

bridges.

ACKNOWLEDGEMENT

This study was partly supported by the Grant-in Aid for Scientific Research from the Japanese Ministry of Education, Science and Culture. Much help from Dr. M. Kato, Mr. Y. Ishiguro and Mr. Ma Zhiliang of Nagoya University is highly appreciated.

REFERENCE

1) Japan Road Association, Standard Specification for Highway Bridges, 1980. (in Japanese)
2) NISHIKAWA, K., The Fatigue Problem and Repair and Rehabilitation of Highway Bridges, Bridge and Foundation, Vol.17, No.8, 1983. (in Japanese)
3) IWASAKI, M. et al., Fatigue Cracking in Steel Bridge members and Recommendation of Retrofitting Method, Yokogawa Bridge Works Technical Report, No.18, 1989. (in Japanese)
4) Public Works Research Institute, Ministry of Construction, Loading Test on Kyowa Viaduct, PWRI Report No.2123, 1984. (in Japanese)
5) Public Works Research Institute, Ministry of Construction, Measurement of Stress Histogram on Composite Bridge with Fatigue Damage, PWRI Report No.2344, 1986. (in Japanese)
6) Public Works Research Institute, Ministry of Construction, Investigation on Durability and Rehabilitation of Existing Bridges, PWRI Report No.2420, 1986. (in Japanese)
7)British Standard Institution: Steel, Concrete and Composite Bridges, Part 10, Code of practice for Fatigue, 1980.
8) European Convention for Constructional Steelwork: ECCS Recommendations for the Fatigue Design of Steel Structures, 1985.
9) YAMADA, K. and MIKI, C.; Recent Research on Fatigue of Bridge Structure in Japan, Journal of Constructional Steel Research, Vol.13, 1989.

Theoretical Evaluation of Remaining Fatigue Life of Steel Bridges

Evaluation théorique de la durée de vie restante de ponts en acier

Theoretische Abschätzung der Restlebensdauer von Stahlbrücken

Annibale Luigi MATERAZZI
Civil Engineer
University of Rome
Rome, Italy

Annibale Luigi Materazzi received his civil engineering degree at the University of Rome in 1977. In 1986 he earned the degree of «Dottore di Ricerca». His research interests are in the fields of fatigue of bridges and offshore structures and fracture mechanics of concrete.

Emanuele F. RADOGNE
Professor
University of Rome
Rome, Italy

Emanuele Radogne, born 1930, directs research work into the dynamic response of structures in service, probabilistic analyses, problems of fracture mechanics of concrete, and redesign of concrete structures.

SUMMARY
An operative methodology for the assessment of remaining fatigue life of existing railway bridges is presented. Either the Miner rule or the Paris crack propagation law can be used. Examples are provided in order to show the method's sensitivity to variation of input data. A critical examination of the results leads to justification for field measurements of structural response.

RÉSUMÉ
L'article présente une méthode d'évaluation de la durée de vie restante de ponts de chemin de fer existants en acier. Cette méthode permet aussi bien l'application de la loi de Miner que celle de la loi de Paris pour la propagation de fissures. Quelques applications numériques sont présentées ensuite afin de montrer la sensibilité de la méthode par rapport à la variation des données. Un examen critique des résultats justifie les mesures sur la structure.

ZUSAMMENFASSUNG
Vorgestellt wird eine operationelle Methode zur Abschätzung der Restlebensdauer bestehender Eisenbahnbrücken aus Stahl. Hierfür eignen sich sowohl das Verfahren von Miner als auch die Gleichung von Paris für das Risswachstum. Anhand von Beispielen wird die Empfindlichkeit der Methode für Änderungen der Eingabe-Parameter gezeigt. Eine kritische Prüfung der Resultate rechtfertigt die Durchführung von Messungen im Feld.

1. INTRODUCTION

In the recent years the attention toward durability has considerably increased, as many structures are approaching the end of their service lives and damages due to materials' deterioration are reported [1]. In this frame the problem of the evaluation of the fatigue damage and of the corresponding ramaining life begins to set up concretely, especially in the case of the bridges.
The analytical procedure for the evaluation of remaining fatigue life has been well known for a long time [2,3] but its practical application demands for reliable data and probabilistic methods.
In the present paper the attention is paid to the case of steel railway bridges because in these structures it is often possible to detect the fatigue cracking and to known with better approximation the magnitude and the cycles' number of past loads.

2. STATEMENT OF THE PROBLEM

In the present paper the problem of the evaluation of residual life is dealt with at Level 2, for an assigned value of the safety index ß, with reference to a steel railway bridge. The structure is supposed to have been designed for fatigue with the criteria of Eurocode 3 [4].
It is in general possible to get additional information on the time history of the stress cycles in service, by means of strain measurements. The measures must be carried out during time intervals long enough to make possible the delicate process of extrapolation of measured data to the whole future life of the bridge.
In this phase it is also necessary to set the correspondence between number of cycles and duration of time. It is often possible to examine in situ the hot spots of steel structure, in order to detect the presence and the length of eventual fatigue cracks by means of suited instruments .
The evaluation of the residual life is performed at an assigned time T, which corresponds to a known fraction of the duration of the design life. The stress collective, on the basis of field measurements, is assumed to be different from the one used at the time of the design. The corresponding damage is computed applying the Miner rule.
Then the influence of the load sequence is investigated applying the Paris law.
The comparison of the numerical results encourages in carrying out in situ strain measurements, in order to improve the knowledge of the stress collective.

3. THE EVALUATION OF RESIDUAL LIFE

In the frame of the Level 2 methods for the assessment of safety, the residual fatigue life may be expressed as:

$$T_{res} = T_{res}(\mathbf{X}, ß_0) \tag{1}$$

where T_{res} is the duration of the residual life, $\mathbf{X}$ is the m-component vector of the design variables and $ß_0$ is the prescribed value of the safety index.
If the problem parameters are:

$$\mathbf{X} = \{T_{past}, \Delta\sigma_{past}(t), \Delta\sigma_{fut}(t), R(N)\}^T \tag{2}$$

where T_{past} is the duration of the past life, $\Delta\sigma_{past}(t)$ is the time history stress cycles applyed in the past, $\Delta\sigma_{fut}(t)$ is the time history of future stress cycles, $R(N)$ is the law of fatigue behaviour of material, then the (1) reduces to:

$$T_{res} = T_{res}(T_{past}, \Delta\sigma_{past}(t), \Delta\sigma_{fut}(t), R(N), ß_0) \tag{3}$$

Everyone of these parameters, except β_0, is in general a random variable. The safety index β depends on the same parameters and on T_{res}:

$$\beta = \beta(T_{res}, T_{past}, \Delta\sigma_{past}(t), \Delta\sigma_{fut}(t), R(N)) \tag{4}$$

The solution of the eq. (1) may be found by iteration solving the (4) in the form $\beta = \beta_0$. The (4) expresses a conventional Level 2 safety problem. Its solution requires to write down the limit state condition in the case of fatigue failure $Z(\underline{X})=0$. If the fatigue damage is computed using the Miner rule, then it is particularly simple:

$$Z = \Delta - \sum_{i=1}^{k} \frac{n_i}{N_i} = 0 \tag{5}$$

where n_i is the number of the stress cycles having amplitude $\Delta\sigma_i$, N_i is the number of the stress cycles of the same amplitude which would lead to failure and Δ is the ultimate value of the damage.
If the Paris law is used to evaluate the propagation of a critical fatigue crack, the eq. (5) modifies into the:

$$Z = a_f - a \tag{6}$$

where a is the current length of the crack and a_f is the corresponding ultimate value.
Then in both cases the basic variables $\underline{X}$ are transformed in a corresponding set of uncorrelated normal standard variables $\underline{x}$. Also the limit state condition is projected in the space of the variables $\underline{x}$ and becomes $z(\underline{x})=0$.
The limit state condition is approximated by means of an hyper-plane tangent to it in the point nearest to the origin:

$$z(\underline{x}) \approx \sum_{i=1}^{m} \alpha_i x_i + \beta = 0 \tag{7}$$

where $\underline{\alpha}$ is the vector of direction cosines of the normal to that hyper-plane. Then it follows:

$$\beta = -\sum_{i=1}^{m} \alpha_i x_i \tag{8}$$

and β is computed by iteration.
The value of Tres corresponding to $\beta = \beta_0$ is the solution of the eq. (2).

4. SOME REMARKS ON INPUT PARAMETERS

4.1 The stress collective

The time history of the loads applied to a structural component of a steel bridge is a random process, as it is the response to a random load, the traffic. In general it is a wide-banded process, whose power spectral density exhibits several maxima, corresponding to the structural natural modes and to the maxima of input process. In the study of the fatigue phenomena it is useful to know the statistic properties of the stress cycles of the response process.

It is well known that in the case of narrow-banded response the amplitudes of the stress cycles are Rayleigh distributed:

$$p(\Delta\sigma) = (\Delta\sigma)/\mathrm{var}(\Delta\sigma))\exp(-\Delta\sigma 2/2\mathrm{var}(\Delta\sigma)) \quad (9)$$

In the opposite case when the response process is infinitely wide-banded the distribution of the amplitudes is approximately normal.
By means of integration it is possible to find the corresponding stress collective. In the case of narrow band the integration of eq. (9) leads to:

$$N = N_{max}\exp(-\Delta\sigma 2/2\mathrm{var}(\Delta\sigma)) \quad (10)$$

with $N_{max} = vT$, where v is the frequency of the process and T is its duration.
It is easy to see that eq. (10) is a parabola in semilogarithmic scale (Fig.1a).
In the case of wide band the stress collective is computed by numerical integration and shows the trend of Fig.1b.
Also when the distribution of the cycles amplitudes is neither Normal, nor Rayleigh it is necessary to resort to numerical integration.

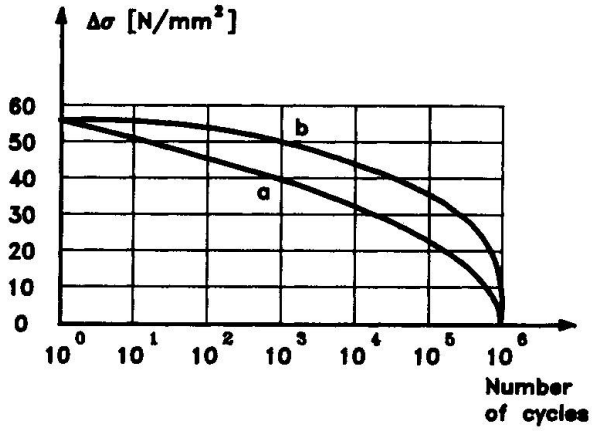

Fig.1 Stress collective: a) narrow band and b) wide band structural response

4.2 The damage criterion

The simplest and most widely used damage criterion for the evaluation of the fatigue life under variable amplitude loading is due to Palmgren e Miner. It expresses the fatigue damage D as:

$$D = \sum_{i=1}^{k} \frac{n_i}{N_i} \quad (11)$$

On the basis of laboratory tests Miner [5] reports that the range of values for D was from 0.61 to 1.49, with an average value close to unity.
In 1954 Marco e Starkey [6] report that in the case of sequences of ascending stress amplitudes the average value for D was 1.49 and in the case of descending loading the average value for D was found to be 0.78. To simulate this behaviour they propose the following non-linear damage criterion:

$$D = \sum_{i=1}^{k} \left(\frac{n_i}{N_i}\right)^{\delta} \quad (12)$$

with δ depending on the order of application of loading blocks.
In the '60 the methods of assessment of damage based on fracture mechanics assert themselves, especially in the field of mechanical engineering. Among the others we remember the Paris - Erdogan law [7]:

$$da/dN = C(\Delta K_I)^n \quad (13)$$

where da/dN is the rate of crack propagation and ΔK_I is the opening mode stress intensity factor. The crack does not grow if ΔK_I is lower than a threshold value K_{IC}. The fatigue failure occurs when the crack length a reaches the critical value a_f. Further improvements to this criterion are due to Klesnil e Lukas [8], who consider the threshold value as a function of the stress history and to Forman, Kearney , Engle [9], who take into account the ratio between the minimum stress and the maximum one in every cycle $R=\sigma min/\sigma max$.
In 1978 Hashin e Rotem [10] propose a non-linear damage criterion which remembers the sequence of stress cycles. It is expressed by the recurrent relation:

$$D = \mu_i \quad (14)$$

$$\mu_i = \mu_{(i-1)}^{A} + n_i/N_i$$

with $A = (\Delta\sigma_i - \Delta\sigma_e)/(\Delta\sigma_{i-1} - \Delta\sigma_e)$
where $\Delta\sigma_e$ is the material endurance limit.

5. NUMERICAL APPLICATIONS

The proposed method of analysis was applied to an actual case, to test its validity and the sensitivity to input parameters.
A steel railway bridge was considered. The evaluation of the remaining fatigue life was performed at a welded joint of a secondary beam of the deck.
As far as the material is concerned, the SN law is assumed to be a straight line in logarithmic scale, without endurance limit, following the equation:

$$N\Delta\sigma^l = B \quad (15)$$

with $l = 5$ and $B = 10^{16}$.
the ordinate at 10^6 cycles is therefore 100 N/mm^2. It corresponds to the mean value minus two standard deviations.
The crack propagation law is the Paris-Erdogan one with $n = 3.3$, $C = 2.43\times10^{-12}$ and $\Delta K_{IC} = 5.8$ MN/$m^{3/2}$. These figures correspond to the mean value of variables.
The stresses applied to the structural member during its past life were extimated to fit into a collective of parabolic shape having a total duration of 100×10^6 cycles and maximum ordinate $\Delta\sigma_{max}$ of 50 N/mm^2. The collective of future stresses was supposed to have the same shape with the same values of duration and maximum ordinate.
The evaluation of fatigue damage was performed using the Miner rule, adopting as its critical value 0.8, as suggested by Augusti [11]. The residual life was computed at Level 2 applying the procedure presented in the chapter 3., for the value $\beta_o=3$ of the safety index. Also the values $\beta_o=2$ and $\beta_o=4$ were considered as a reference. Input data are presented in Table 1.
The analysis led to the following extimates of the residual life T_{res}, expressed as number cycles: for $\beta_o=2$ $T_{res} = 3.30\times10^{10}$, for $\beta_o=3$ $T_{res} = 6.53\times10^{9}$, per $\beta_o=4$ $T_{res} = 1.17\times10^{9}$.
Then a sensitivity analysis was stated, varying some of the most important parameters.
First of all the influence of the mean value of the

random variable	distribution	expected value	c.o.v.
$\Delta\sigma_{max}$	log-normal	50 N/mm^2	0.20
T_{past}	log-normal	10^8 cycles	0.10
$\Delta\sigma_{SN}$	log-normal	167 N/mm^2	0.20
Δ	log-normal	0.8	0.20

Table 1 Input data of the basic case (Miner rule)

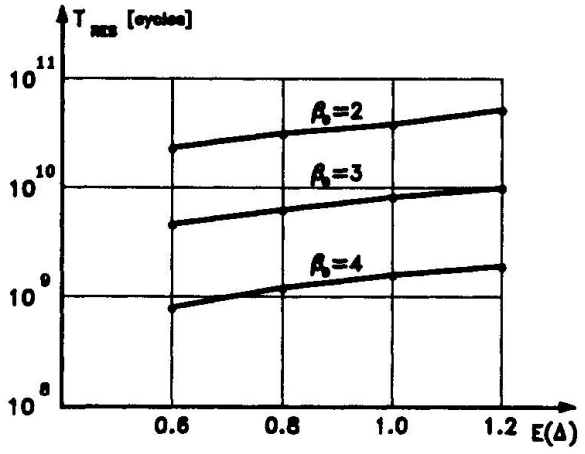

Fig.2 Remaining life as a function of the mean value of the limiting figure of the Miner sum

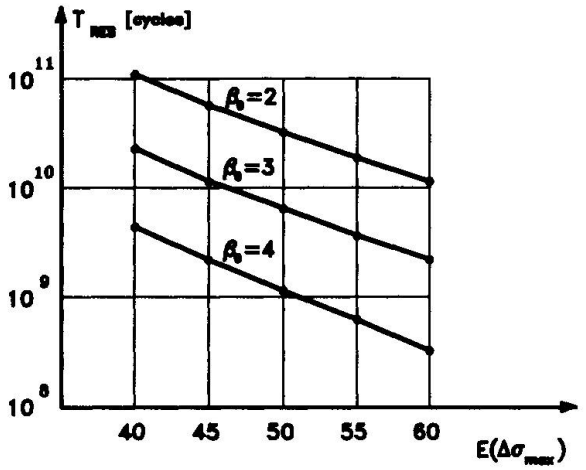

Fig.3 Remaining life as a function of the mean value of $\Delta\sigma_{max}$ expressed in N/mm^2

limiting value of the Miner sum was examined, varying it in the range between 0.6 and 1.2.

The corresponding results are reported in Fig.2. In all the three cases considered for β_0 a nearly twofold variation of the residual life was found between the most favorable case and the least one.

Then the influence of the parameters relating to the stress collective of the past was investigated. In the Figs. 3 and 4 the results of the sensitivity tests toward the variation of the expected value of $\Delta\sigma_{max}$ and of its coefficient of variation $V(\Delta\sigma_{max})$ are reported. For the mean value a range between 40 e 60 N/mm^2 was assumed. It lead to variations of about ten times on the evaluation of the residual life for all the three cases of β_0. As far as the coefficient of variation is concerned, value ranging between 0.10 and 0.25 were considered. The corresponding variation on the residual life was 3.4 times for β_0=2, 5.2 times for β_0=3 and 11 times for β_0=4.

Then the sensitivity to the duration of the past life was investigated, separately considering the effect of its mean value variation (Fig.5) and of the c.o.v variation (Fig.6). The mean value varyed between 10^6 and 10^9 cycles. For β_0=2 and β_0=3 a reduced sensitivity was found and for β_0=4 a sensitivity was found only for very high number of cycles, near 10^9.

As far as the coefficient of variation is concerned (investigated range: 0.1 to 0.25), very little sensitivity was found for all the figures of β_0 considered.

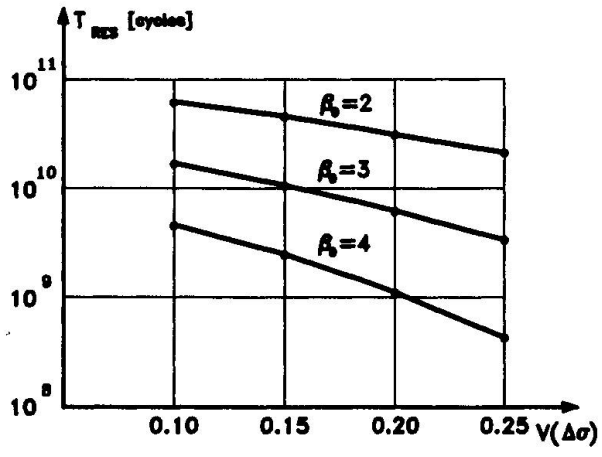

Fig.4 Remaining life as a function of the c.o.v. of $\Delta\sigma_{max}$

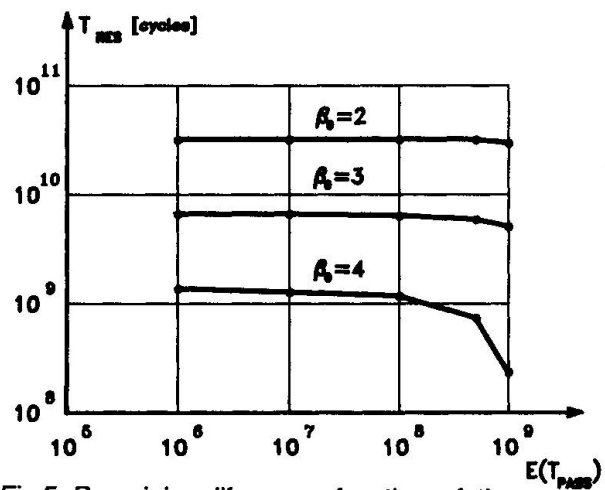

Fig.5 Remaining life as a function of the mean value of the past life

At the end of this part of the investigation the case of simultaneous variation of all input data was considered: first in the most favorable direction, then in the least favorable. The results are reported in Table 2.
Then an analysis of residual life was carried out applying the Paris-Erdogan law Input data are presented in Table 3 and the results are reported in Fig.7.
The numerical computations were performed under two different hypotheses of load application: ascending loading and descending loading. Four values of the initial crack length were also considered: 2,3,4,5 mm.

Case	$\beta = 2$	$\beta = 3$	$\beta = 4$
the most favorable	3.44×10^{11}	9.77×10^{10}	2.76×10^{10}
the basic case	3.30×10^{10}	6.53×10^{9}	1.17×10^{9}
the least favorable	4.36×10^{9}	0.0	0.0

Table 2 Duration of the remaining life expressed as number of cycles

random variable	distribution	expected value	c.o.v.
$\Delta\sigma_{max}$	normal	50 N/mm^2	0.20
C	normal	1.43×10^{-12}	0.10
a_f	normal	40 mm	0.10

Table 3 Input data of the basic case (Paris law)

6. COMMENTS ON THE NUMERICAL RESULTS

Examining the results of numerical computations we can observe that the selected figure for β_0 has a great influence. In fact changing from the value 3.0, which is suggested by the Joint Committee on Structural Safety [12] and is the basic value of our analyses, to 2 the residual life increases an average 5 times and changing to 4 the life reduces an average 5 times.
During the numerical analysis the influence of the parameters describing the stress collective and of the limiting value of the Miner sum was investigated. The major sources of uncertainty are the mean value of the maximum stress range, its coefficient of variation and the damage criterion.
The idea rises from this to reduce the sources of uncertainties with experimental in situ observations oriented toward two directions. The first one is to detect

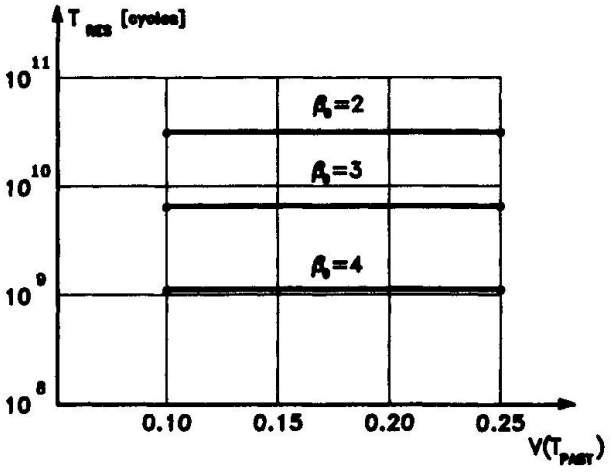

Fig.6 Remaining life as a function of the c.o.v. of the past life

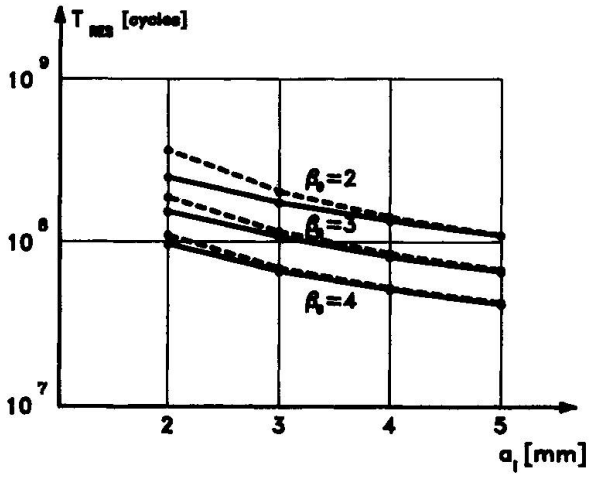

Fig.7 Remaining life computed with the Paris law: continuous line decreasing load, dashed line increasing load. ai is the initial value of the fatigue crack

the fatigue damage of the material by means of the measurement of the length of fatigue cracks. The second one is to improve the extimate of future stress history by means of sampling observations of bridge vibrations, extended to time intervals sufficient to warrant measure stationarity.
The application of the Miner rule with the improved data leads to better results. An alternative way is to use the Paris law, which allows to directly use load data without statistical reordering and the results of damage measurements.
The presented methodology is well suited to be a consistent procedure for the calibration of partial safety factors employed by the Level 1 methods.

7. CONCLUSIONS

The previous examination showed the differences between the procedures for the safety analysis of brand new structures and the existing ones. The first are methods connected to conventional probabilistic models and are intended to be support for the design process, the second ones can take advantage of experimental in situ tests that give improved information on the structural behaviour. Also in the case of fatigue problems it is often possible to gain better information whether using the Miner rule or applying the Paris law.
The theoretical fundamentals of the estimate of the residual fatigue life at Level 2 were reviewed.
The numerical experiments, which were carried out with reference to the case of a steel railway bridge, showed that the application of the method based on the Miner rule leads to estimates highly dependent on the uncertainties enbedded into the parameters that describe the past stress collective. This result encourages to undertake field tests to ascertain the damage accumulated in the past.
The use of the method based on fracture mechanics allow to improve the estimate quality and to take advantage of the information from field control of structural behaviour.
Than it seems reasonable the suggestion to subject the steel railway bridges to periodic control in order to detect incipient fatigue damage and to progressively update the evaluation of residual life. So it is possible to plan eventual strengthening works.

REFERENCES

1. MACCHI G., RADOGNA E.F., MATERAZZI A.L., Synergetic effects of environments actions and fatigue. IABSE Symposium "Durability of structures", Lisbon, 1989, pp. 493-8.

2. HIRT M. A., Remaining fatigue life of bridges. IABSE Symposium "Mainteinance, Repair and Rehabilitation of Bridges", Washington, D.C., 1982, pp. 113-29.

3. STIER W., STEINHARDT O., VALTINAT G., KOSTEAS D., Residual fatigue life of railway bridges. IABSE Colloquium "Fatigue of steel and concrete structures", Lausanne, 1982, pp. 823-31.

4. COMMISSION OF THE EUROPEAN COMMUNITIES, Eurocode No.3: Common unified rules for steel structures, 1984.

5. MINER M. A., Cumulative damage in fatigue. ASME Journal of Applied Mechanics, Vol.12, 1945,pp. A159-A164.

6. MARCO S. M., STARKEY W. L., A concept of fatigue damage. Transactions of the ASME, Vol 76, 1954, pp. 627-32.

7. PARIS P., ERDOGAN F., A critical analysis of crack propagation laws. ASME Journal of Basic Engineering, dec. 1963, pp. 528-34.

8. KLESNIL M., LUKAS P., Influence of strength and stress history on growth and stabilisation of fatigue cracks. Engineering fracture mechanics, Vol. 4, 1972, pp. 77-92.

9. FORMAN R.G., KEARNEY V.E., ENGLE R.M., Numerical analysis of crack propagation in cyclic-loaded structures. Journal of Basic Engineering, Trans. ASME, Sept. 1967, pp. 459-64.

10.HASHIN Z., ROTEM A., A cumulative damage theory of fatigue failure. Materials science and engineering, Vol. 34, 1978, pp. 147-60.

11.AUGUSTI G., BARATTA A., CASCIATI F., Probabilistic methods in structural engineering. Chapman and Hall, London, 1984.

12.DITLEVSEN O., MADSEN H.O., Proposal for a code for the direct use of reliability methods in structural design. Joint Committee on Structural Safety, Working Document, Nov. 1989.

Leere Seite
Blank page
Page vide

Safe Life Evaluation of Existing Bridges

Evaluation conservatrice de la durée de vie des ponts existants

Bestimmung der sicheren Lebensdauer bestehender Brücken

Fred MOSES
Prof. of Civil Eng.
Case Western Reserve Univ.
Cleveland, OH, USA

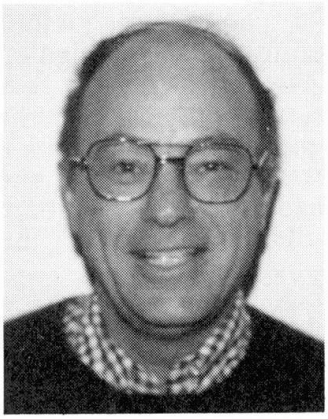

Fred Moses received a civil engineering degree from CUNY in 1960 and a PhD from Cornell in 1963. Since joining Case Institute, Professor Moses has been active in structural optimization and reliability with special applications to bridge and offshore structures including loading, safety analysis and system reliability studies.

SUMMARY

Estimates of the safe remaining life of existing steel bridges affect decisions on inspection, maintenance, replacement, truck weight, permit posting limits and even changes in new weight regulations. A reliability model has been developed and calibrated to produce uniform and consistent fatigue checking procedures for different spans, geometrics, bridge types, and traffic. These methods have been adopted in recent AASHTO Guide Specifications for fatigue design of new bridges and safe-life evaluation of existing steel bridges. The same model has been extended to compute costs associated with proposed truck-weight regulations. These costs affect new designs and particularly, existing estimates of bridge repair and damage.

RÉSUMÉ

L'évaluation de la sécurité des ponts en acier existants influence les décisions relatives à l'inspection, la maintenance, le remplacement, le poids des camions, les limites de charge à imposer, et peut même engendrer des modifications dans les lois réglant le poids des camions. Un modèle de charge a été développé et calibré afin de conduire à des vérifications à la fatigue uniformes et cohérentes pour différentes portées, géométries, types de ponts et trafics. Ces méthodes ont été adoptées dans les nouvelles recommandations AASHTO pour la conception à la fatigue des nouveaux ponts et l'évaluation de la sécurité des ponts en acier existants. Ce même modèle a été étendu afin d'estimer les coûts liés aux propositions de règlements pour le poids des camions. Ces coûts influencent la conception actuelle et, plus particulièrement, les estimations des réparations et du dommage de ponts existants.

ZUSAMMENFASSUNG

Die Abschätzung der sicheren Restlebensdauer bestehender Stahlbrücken beeinflusst Entscheidungen betreffend Inspektion, Unterhaltung oder Ersatz einer Brücke, betreffend signalisierte Gewichtslimiten oder Änderungen der gesetzlichen Gewichtsbeschränkungen. Ein Modell zur Bestimmung der Ermüdungssicherheit von Stahlbrücken wurde entwickelt. Es wurde so angepasst, dass es in einheitlicher Art und Weise für verschiedene Brückentypen, Spannweiten, Geometrien und Verkehrsmischungen anwendbar bleibt. Die Methode wurde in den kürzlich erschienenen AASHTO-Empfehlungen für die Ermüdungsbemessung neuer Brücken und die Bestimmung der sicheren Lebensdauer bestehender Stahlbrücken übernommen. Dasselbe Modell wurde mit dem Ziel erweitert, die Kosten zu berechnen, welche durch Änderungen der Gewichtsbeschränkungen verursacht werden. Betroffen durch solche Änderungen sind die Kosten neuer Konstruktionen und, in vermehrtem Masse, die Reparaturkosten bestehender Brücken.

1. INTRODUCTION

A companion paper describes a reliability-oriented load prediction model for the random fatigue damage accumulation per year [1]. This damage was expressed in terms of traffic, material and analysis random variables. The data base was expressed in terms of nominal values and bias and respective coefficients of variation. The study described in this paper utilizes the probabilistic damage accumulation and data base to determine safety indices for fatigue failure modes. These safety indices are used to calibrate fatigue procedures for evaluation. These procedures contain nominal checking procedures and factors of safety for both redundant and nonredundant load path structures. The aim is to have uniform and consistent safety indices over the full range of traffic spectra, bridge types and spans. These methods have been incorporated into two recently adopted AASHTO Guide Specifications for design of new steel bridges and safe life evaluation of existing steel bridges [2,3]. Assessment of safe remaining fatigue life is useful for developing inspection intervals, scheduling repair and replacement and making permit decisions. A second application of the fatigue risk model is the extension to a cost allocation study of new truck weight regulations. Projected increases in truck weight and volume changes affect the cost of fatigue damages. Projections were made using the reliability model to the remaining life and costs for over 70,000 steel bridges in the United States over the coming 50-year period [4].

2. FATIGUE RELIABILITY MODEL

This section formulates a reliability approach to predict that the fatigue life of steel beam attachments will be less than the estimated life. Several points to note are: (1) the assumptions of the model, (2) the random variables in the true fatigue life, and (3) the sensitivity of the risk to the statistical parameters of these random variables. The safety margin is expressed in terms of a failure function, g, as in usual structural reliability practice.

$$g = Y_F - Y_S \tag{1}$$

Failure does not occur if $g < 0$. Y_F is life at which failure occurs (a random variable), and Y_S is specified life (deterministic). The expression for Y_F is given in the other paper.

2.1 Safety Index

The safety index (or beta) is the number of standard deviations between the mean of g and the boundary of the safe value of g. If g is normal, the risks corresponding to β are found from a normal probability table, e.g. $\beta = 3$ gives a risk of 0.001. Beta typically falls in the 1 to 4 range in most structural applications. If the variables are not normal, computer programs are available to compute β for general distributions of random variables and failure functions g. The programs output the safety index, β, and the most likely failure values. The latter helps assess in the failure event each random variable. The accuracy in characterizing the statistics of any single variable will decrease as the total number of variables increase as, say, in the fatigue model which has ten random variables. Thus, if we seek a risk of 10^{-4}, the design point value for each variable may fall in only the 10^{-2} range. Thus, realistic and accurate assessments of reliability can be made without requiring an unrealistic amount of data.

2.2 Calibration

Code writers have a responsibility in selecting a consistent target safety index, or β, for a code check. One approach is to base the decision on economics, i.e., an optimum failure rate occurs when the cost trade-off of increasing the safety factor balances the risk reduction of future failures. A problem here is expressing the cost of failure. Another approach is to compile historical failure rates. If the rate is deemed acceptable, this can be considered the societal target

risk. A difficulty is to isolate failures truly related to code checks. Most structural failures occur because of blunders or gross errors in design concept, detailing or fabrication and are *not* related to the code checking. The approach usually adopted for establishing the target beta is to assess the present design provisions and perform safety index calculations over a wide range of representative practice (e.g., for different bridge spans, geometries, attachments). In general, there will be a wide range observed in computed β's because uncertainties were not consistently considered in the original development of the specifications. The aim in any new code provisions should be uniform or consistent target reliabilities. Thus, an average beta based on present standards is selected and this becomes the target for future code provisions.

2.3 Selection of Safety Factors

Figure 1 shows the beta vs. safety factor, γ, for a 100' span bridge and category C detail. The figure was obtained by substituting value a of γ in the expression for fatigue damage (Eq. 22 of Ref. 1) and computing the corresponding safety index, β using Eq. 1 herein. Plots similar to Figure 1 were made for different spans, and different fatigue detail attachments [5]. It was shown that the plot of β vs. γ is not sensitive to such changes so a single representative curve such as Figure 1 could be used. In the calibration, the target beta is selected as an average of the betas implicit in present design practice.

Fourteen AASHTO design cases (A-N) with different truck volumes, detail categories, spans impact factors, lateral distribution factors, and support conditions (simply supported or continuous) are shown in Table 1 to evaluate an average beta implicit in the present AASHTO design practice. This is done by taking sections which just satisfy the present AASHTO fatigue criteria and computing the implicit safety factor, γ. The designs selected were intended to be both representative of typical cases and also to represent possible extreme occurrences. For example, case H has a mean impact of 1.20 and a mean girder distribution of 0.50. The corresponding β's found from the γ versus β graph for each case are shown in Table 1. For example, for redundant or multiple load path members, Table 1 shows, that most of the design points fall around a beta of 2.0. This is midway in the range of the betas (0.7-3.6) corresponding to all the design points. The average β of 2.0 corresponds in Figure 1 to a reliability factor γ of 1.35. The same analysis was repeated for nonredundant details. The mean of the range of betas (1.5-5.3) for nonredundant details appears to be about 3.0. This corresponds to a reliability factor, γ, of 1.75. From this analysis of the average betas for existing design the target safety index for redundant and nonredundant members was fixed as 2.0 and 3.0, respectively, in the proposed evaluation procedure.

These examples demonstrate quite strongly the advantages of the proposed format. For redundant spans, we try and achieve our target β of 2 for all the design cases while AASHTO produced betas ranging from 0.7 to 3.6. Design with high betas is uneconomical, while the low betas will have relatively low probabilities that the actual fatigue life will exceed the predicted life. Similarly, for the non-redundant cases, the proposed evaluation methods try to achieve a target β of 3.0 for all cases compared to AASHTO betas that range from 1.5 to 5.3. The target betas will not be achieved exactly even for the proposed procedures. More factors would be needed to make this possible. The scatter in beta, however, will be smaller. The corresponding betas for these sections are shown in columns (5) and (7) of Table 1 for redundant and nonredundant members, respectively. The scatter in beta for redundant members is between 1.85 and 2.17 (as against 0.7 to 3.6 for AASHTO methods) and for nonredundant members it is between 2.85 and 3.10 (as against 1.5 to 5.3 for AASHTO methods). Hence, the proposed procedures achieve the goals of a more uniform safety index.

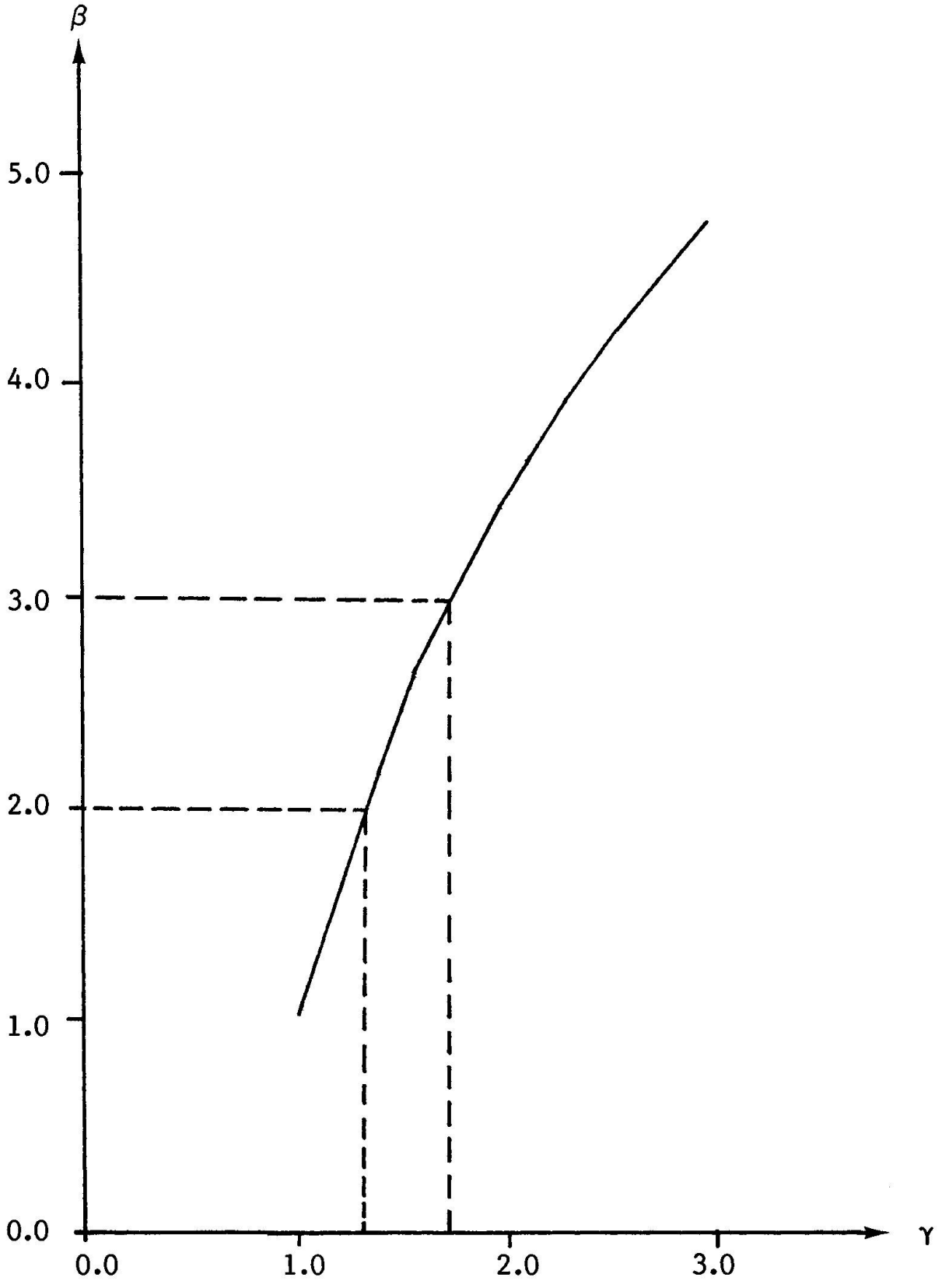

Figure 1. Mean γ vs. β curve.

2.4 Safety Factor Adjustments in Evaluation Procedure

The evaluation procedures have been developed with the following aims: (1) consistent and uniform reliability over the range of application (all spans, categories, lives, volumes); (2) flexible to incorporate site-specific data; (3) flexible to provide the Engineer with a better (usually longer) fatigue life estimate if more effort is applied. The first aim was satisfied by the calibration process. A target safety index has been fixed to achieve consistent and uniform reliability. The other two goals are obtained by incorporating several alternatives to the basic procedure. Some of the alternatives need site-specific data, while some other alternatives require more analysis effort by the Engineer. It should also be noted that in the evaluation, the Engineer can also obtain the mean fatigue life as well as the safe life. This should help explain why a span, which does not satisfy a safe life check, may not show any visual signs of fatigue cracking. Typically, the mean life will be about 5 times the computed safe life for redundant spans and 10 times the safe life for nonredundant spans. For a span not meeting the required safe life, the Engineer can select different options including more frequent inspection or control on vehicles.

Most of the alternatives in the evaluation lead to lower safety factors. The concept here is that risk is influenced by both the safety factor and the uncertainty. The same target safety index can therefore be achieved by reducing uncertainties and using a smaller safety factor. For example, availability of stress measurements for an attachment rather than the computed value permit the reliability factors, γ, to be reduced by 0.85. Use of measured truck weight spectra to provide a site-specific equivalent effective weight for the fatigue design vehicle reduces the γ's by 0.95. Finite element analysis to compute attachment stresses rather than the distribution chart or formulas provided in the specification reduce γ's by a factor 0.96.

2.5 Fatigue Limit

It is generally accepted that a constant amplitude fatigue limit exists for typical bridge details. If all cycles in a variable amplitude spectrum are below this constant amplitude fatigue limit, the fatigue life for the spectrum would be infinite. More research is still required to determine if a fatigue limit exists for a variable amplitude stress spectrum when only several stress cycles exceed the constant amplitude fatigue limit. Long life fatigue tests being conducted at Lehigh, TRRL, Maryland, and elsewhere may help resolve this issue. As one illustration,the reliability program was modified to exclude all the stress cycles below the constant amplitude fatigue limit while computing the fatigue damage. The results show that even after the model has been changed (a fatigue limit is introduced), the average betas from the proposed method and the AASHTO method are still almost the same [5].

3. PROPOSED FATIGUE EVALUATION PROCEDURES

A proposed bridge fatigue evaluation procedure based on the above reliability analysis was approved as a Guide Specification by AASHTO. Although optional as a requirement, it is being developed for a new edition of the commonly used AASHTO Maintenance Inspection Manual. This document is used to evaluate on a two year cycle, each of the nation's 600,000 bridges. The fatigue evaluation specification is primarily intended to determine the remaining safe life for application to inspection, maintenance, repair, replacement strategies, permit review and general truck weight control policies.

3.1 Application

This section summarizes the recently approved AASHTO Guide Specifications for fatigue evaluation of steel bridges [3]. The specifications for assessing remaining safe life apply only to uncracked members subjected to primary stresses that are normally calculated in design. The

stress range is calculated first and used to predict the remaining mean and safe fatigue lives. The remaining mean life is the best possible estimate of the actual remaining life. The remaining safe life is a more conservative estimate which provide a level of reliability comparable to present AASHTO fatigue provisions. Alternatives that may be used at the option of the Engineer are given for several steps in the procedure. Each attachment must be considered individually.

The stress range for fatigue evaluation can be calculated by the following steps or, alternatively, can be determined from field measurements. A fatigue truck is used to represent the variety of trucks of different types and weights in the actual traffic. This truck has three axles with axle spacings of 14 ft and 30 ft and axle weights of 6, 24 and 24 kips respectively. This spacing approximates that for the 4- and 5-axle semitrailers that do most of the fatigue damage to bridges. The gross weight of the fatigue truck is 54 kip; this weight was developed from extensive weigh-in-motion data. Alternatively, the gross weight can be calculated from a truck-weight histogram obtained from weigh station or weigh-in-motion data for the site. Alternative axle spacings and weight distributions based on site data are also permitted.

The effects of more than one truck on the bridge at a time can be neglected unless there are conditions of close spacing of the trucks. The dynamic impact caused by different trucks usually vary considerably. Test data indicate that a factor of 10 percent is appropriate for fatigue evaluations. Poor joint or pavement conditions, however, require higher values.

The stress range is based on the moment or axial load range caused by the passage of the fatigue truck across the bridge. The lateral distribution factors for the fatigue evaluation are based on a single truck at the centerline of a traffic lane rather than on trucks in all lanes. Field tests have shown that the bending stress of actual bridge members is below that calculated by normal procedures, which conservatively neglect such effects as unintended composite action, contributions from nonstructural elements such as parapets, unintended partial end fixity at abutments, and direct transfer of load through the slab to the supports. To account for these effects, the computed section modulus is increased by appropriate percentages for composite and noncomposite sections, respectively.

Reliability factors are provided to assure adequate reliability in calculating the remaining safe life for different cases. Basic factors are recommended for redundant and nonredundant members. The corresponding probabilities that the actual remaining fatigue life will exceed the calculated remaining safe life are about 97.7 percent and 99.9 percent, respectively. The reliability factor is 1.0 for calculating the remaining mean life. If the compressive dead load stress is high enough so that essentially all of the stress cycles caused by normal traffic are completely in compression, the fatigue life is assumed to be infinite. If the maximum stress range in tension falls below the fatigue limit for a particular detail, crack growth will not occur and infinite fatigue life may be assumed. This situation, which applies primarily to higher detail categories (C and above), is checked by comparing the factored stress range with a fatigue limit value calibrated to a β of 2 to provide an adequate reliability that crack initiation will not occur. This fatigue limit value is equal to (1/2.75) times the present AASHTO allowable stress range for the over-two-million cycle category.

Finite remaining life: If a given detail does not satisfy the infinite life check, the remaining safe fatigue life (in years) corresponding to the factored stress range is calculated for a lifetime average truck volume and a selected number of stress cycles per truck passage. Alternatively, more refined procedures that involve growth rates and changes in truck weights with time can be used to calculate the remaining fatigue life. Detail constants are for the detail categories in the present AASHTO specifications. The equivalent number of stress cycles per truck passage is given for various cases.

Options if remaining life is inadequate: The evaluation procedure gives four options that may be pursued if the Engineer considers the calculated remaining safe fatigue life to be inadequate. These include (1) calculating fatigue life more accurately, (2) restricting traffic on the bridge, (3) repairing the bridge, or (4) instituting periodic inspections.

4. EVALUATION OF PROPOSED TRUCK WEIGHT REGULATIONS

In most industrialized countries there is increasing economic and political pressures to allow heavier vehicles and special permit trucks. The productivity gains are impressive from such weight increases and pavement damage can be mitigated or reduced by allowing vehicles with up to nine or more axles. A recent Bridge Impact Study by the writer was conducted for the Transportation Research Board under a congressionally mandated truck weight study [4]. It is only for bridges that increased truck weights may cause damages which offset the expected gains to freight shippers. Most of the bridge cost concerns strength capacity and increasing numbers of structurally deficient bridges. Fatigue costs were also considered. The approach used in the study is a reliability model similar to that given above for fatigue evaluation. This model gives the increasing risk of fatigue cracking as a bridge ages and accounts for different truck spectra. The probability that the actual fatigue life will be less than current life can be obtained from the reliability index.

4.1 Fatigue Damage

Fatigue damage is caused by all trucks passing over the bridge. If present truck weight regulations are changed, a percentage of the trucks in present traffic will be replaced by the new heavier trucks permitted. To calculate the relative fatigue damage caused by traffic before and after the change, it is necessary to know the composition of the truck traffic before and after the change; that is, the percentages of different types and weights of trucks in the traffic. In essence, the proposed fatigue cost model projects present expenditures for fatigue problems in steel bridges and adjusts these costs based on changes in traffic projections and passage of time.

4.2 Present Fatigue Cost

An estimate of the present expenditures on fatigue problems is required so that they can be used as a base case in projecting the expenditures associated with new truck weight scenarios. A limitation in a state survey is that agencies generally have great difficulty in assessing the costs of fatigue damage and relating these to vehicle regulations. In addition to the state survey, an estimate of the current annual cost of fatigue damage on steel structures in the United States was discussed with several experts on fatigue damage and repairs in highway bridges. For example, Dr. John Fisher stated that he has personal knowledge of fatigue problems on several hundred bridges. Based on these discussions an annual figure of $50 million would be an appropriate estimate. These include all costs to (a) repair actual or potential fatigue damage, (b) replace bridges that are unsafe because of fatigue damage and cannot be economically repaired, (c) perform engineering studies to evaluate actual or potential fatigue problems revealed by routine inspections or suggested by experience with similar bridges at other sites, (d) make engineering studies to develop appropriate corrective measures if required, (e) make extra inspections required to monitor fatigue cracking or check certain types of bridges that have had fatigue problems at other sites, and (f) reroute traffic when a bridge is closed because of fatigue problems.

Over the next 50 years, $50 million per year of damage (present value) totals $2.5 billion. There are 75,000 steel bridges on Interstate and primary routes and $2.5 billion in damage represents about 12% of the net value of such structures. This percentage is not unreasonable since present AASHTO fatigue design procedures are based on a 5% exceedance probability for fatigue life

failure and further, many steel bridges were constructed before any fatigue provisions were in place and in recent years there has been significant increases in truck volume and average weight.

4.3 Future Fatigue Costs

The fatigue risk model is used to extrapolate the present fatigue damage costs as they increase in the future due to a) passage of time and accumulation of more cycles of loading, and b) changes in weight regulations which accelerate the damage rate. For different weight changes or scenarios the costs are found by computing fatigue cost vs. a damage ratio, R. The reference or base value for cost is \$50 million per year. The damage ratio, R, is defined as:

$$R = \Sigma_i P_i R_i \tag{2}$$

where i - indicates span interval (including both simple and continuous spans)
P_i - percent of steel bridges in span interval i
R_i - applicable damage ratio for interval i.

$$R_i = \frac{\Sigma_t \Sigma_W V(t,W,S)\, M(i,t,W,S)^3}{\Sigma_t \Sigma_W V(t,W,B)\, M(i,t,W,B)^3} \tag{3}$$

where t - truck vehicle type
W - weight interval for truck type t
$V(t,W,S)$ - volume for truck type t, weight interval W, and proposed truck weight scenario S
$M(i,t,W,S)$ - maximum bending moment for span i, for weight W, and type t, in scenario S
$V(t,W,B)$ - base case (current) volume for type t, weight interval W
$M(i,t,W,B)$ - corresponding moments for base case

4.4 Future Damage

In the bridge evaluation, the reliability model is applied to a single bridge (with known design life and site parameters). The approach now is to extrapolate to the entire system of existing bridges. An average present life of 25 years was used as typical for existing Interstate and major route structures that are affected by fatigue problems. New weight regulations change the rate of "aging". A parameter y is used to express future damage, D_f, in terms of present damage, D_0.

$$D_f = D_0 \frac{25 + (AGE - 25)\, R}{25} = D_0 y \tag{4}$$

Where y = aging parameter
AGE = average bridge age at a future time compared to present 25 year age.
R = ratio of the annual damage after new weight regulations to present annual damage from Eq. (2).
D_0 = damage accumulated at present
D_f = damage accumulated at future date

R is the ratio of damage before and after a change in truck weight regulations and accounts for both truck weight and volume changes. A productivity analysis was part of the truck weight study to project volume changes within each truck type and region in the U.S. Because of the wide range of design loadings and truck volumes for the population of existing bridges, the fatigue risk procedure must be calibrated for the average safety margin of the entire population. Based on the number of fatigue problems to date, a beta of 2.5 seems reasonable. This implies a

probability of 0.006 for a fatigue failure on an existing bridge. A .006 risk would mean 450 fatigue failure. This is plausible in view of Professor John Fisher's comment above.

Using a β = 2.5, y = 1 (present age) and the risk model in Eq. (1) leads to a mean safety margin of 14. This means that the typical bridge has an expected life 14 times the present average life of 25 years. As the structure ages, and further damage is accumulated, beta decreases. For example, when beta falls to 1.5 in the future the risk for an average steel bridge will have increased from .006 (at the present time) to about 0.067. This represents an increased risk ratio of 11.2. Using the 75,000 bridge sample, instead of the cumulative 450 failed bridges at present, there is expected to be a cumulative total of 5,025 damaged bridges at that time. It is assumed that damage costs increase in direct proportion to the number of failed bridges. Thus, the total cost at the future time, when beta is 1.5, will be 11.2 times the present $50,000,000 or $560,000,000 per year. In order to compare with productivity benefits future damage costs are transformed to constant equivalent annual costs over the next 50 years.

4.5 Examples

Fifty years of future life are projected to cover the remaining life of the existing population of steel bridges. New steel bridges will be based on the new truck weight regulations to have adequate fatigue life and are not included in this cost analysis. For example, the equivalent uniform annual cost of fatigue damage with no change in present damage rate is $157M/year using i = 7%. If the new truck regulations double the damage ratio, R, to 2.0, the fatigue damage increased to $320M/year. Sensitivity studies were carried out to find the fatigue costs for different assumed present beta, interest rates and other statistical parameters [4].

4.6 Proposed Truck Weight Regulations

It is shown above that the present equivalent annual cost of bridge fatigue damage with no change in regulation is $157M/year. This is based on the fatigue risk model to extrapolate the present expenditures of $50M/year will increase as bridges "age" increasing the risk. Several different weight change scenarios were studied along with data from productivity projections to estimate the volume of truck changes. As a base case, the present U.S. legal truck weight limit is 80,000 lbs although many jurisdictions permit higher weight under special legal, legislative or administrative actions.

Adoption of a proposed Canadian Interprovincial truck regulation, for example, would increase the gross weight from 80,000 to 131,000 on a 65' wheel base as well as other weight increases for shorter wheel base vehicles. The fatigue damage increase using Eq. 2 was found to be R = 1.41 [4]. This raises fatigue damage costs by an estimated $65M/year. In general, it is found that truck weight regulations have a much greater cost impact due to causing strength deficiencies than shortening of fatigue life. Such conclusions assume that funds will be expended to increase strength capacity levels to requirements for increased truck weights. One possibility is that agencies will restrict heavy vehicles to special routes which do not require strength upgrades. In that case, the fatigue cost may be a significant proportion of the total bridge costs. In all, some 20 truck weight scenarios were studied using the FHWA data file of some 600,000 bridges. With respect to all weight regulations studied, productivity gains far outweighed bridge costs.

5. CONCLUSIONS

1. Reliability models are available to develop nominal fatigue checking formats and safety margins which lead to uniform and consistent reliability indices.
2. Sufficient data is now available to calibrate the model to use performance experience as a guide for computing target indices for singe and redundant load path systems.

3. A Guide Specification has been presented and adopted by AASHTO which is based on the model discussed herein and has been extensively used by several agencies.
4. Extensions of the fatigue risk model estimated future bridge damage costs if truck weight regulations permit heavier loadings and more rapid aging of structures.
5. It is important that increased tax revenue be available to the bridge system to ensure adequate funds for increased inspection, repair and eventually earlier replacement.

6. ACKNOWLEDGMENTS

The author acknowledges the contributions of his coworkers on the project, C.S. Schilling and K.S. Raju. Other assistance from I. Friedland and H. Cohen, TRB Contract Managers and Project Consultants, Professor John Fisher and Dr. Abba Lichtenstein are appreciated.

REFERENCES

1. "Bridge Load Models for Fatigue", IABSE Workshop on Remaining Fatigue Life of Steel Structures, Lausanne, 1990.

2. Guide Specifications for Fatigue Design of Steel Bridges, AASHTO, Washington, D.C., 1989.

3. Guide Specifications for Fatigue Evaluation of Steel Bridges, AASHTO, Washington, D.C., 1990.

4. Moses, F., "Effects on Bridges of Alternative Truck Configurations and Weights", NCHRP Contract HR2-16(b) Report to Transportation Research Board, Washington, D.C., December 1989.

5. Moses, F., Schilling, C.G. and Raju, K.S., "Fatigue Evaluation Procedures for Steel Bridges", NCHRP 299, Transportation Research Board, Washington, D.C., 1987.

Table 1 Comparison of β's in proposed methods and present AASHTO methods

			β		β	
		Detail	Redundant Members		Nonredundant Members	
Designation	Span	Category	AASHTO	Proposed	AASHTO	Proposed
(1)	(2)	(3)	(4)	(5)	(6)	(7)
A	120'SIMPLE	C	1.05	1.99	1.85	2.93
B	100'SIMPLE	C	2.00	2.02	2.90	2.96
C	60'SIMPLE	A	2.05	2.03	2.10	2.85
D	60'SIMPLE	B	2.15	1.97	2.65	2.92
E	60'SIMPLE	C	2.20	2.10	3.20	2.93
F	60'SIMPLE	D	2.75	1.97	3.90	2.91
G	60'SIMPLE	E	3.10	1.85	5.35	2.87
H	30'SIMPLE	C	0.70	2.16	1.50	3.09
I	100'CONT	A	1.45	2.06	1.50	2.89
J	100'CONT	B	1.60	2.01	2.00	2.98
K	100'CONT	C	1.65	2.05	2.80	2.99
L	100'CONT	D	2.05	2.01	3.45	2.97
M	100'CONT	E	2.40	1.90	4.80	2.96
N	60'CONT	C	3.55	2.17	4.10	3.10

Accumulation of Fatigue Damage, Automatically Recorded and Evaluated

Cumul du dommage en fatigue: enregistrement et analyse automatiques

Schadensakkumulation infolge Ermüdung: automatische Aufzeichnung und Auswertung

Tomas NAVRATIL
Cybernetics Engineer
Tesla Elstroj
Prague, Czechoslovakia

Tomas Navratil, born 1960, received his M.S. degree at the Czech Technical University in Prague. For six years, he has been interested in control and data acquisition systems as well as software development. At present he is working on his PhD thesis at the Czech Technical University.

Pavel MAREK
Assoc. Prof.
Sportovni stavby
Prague, Czechoslovakia

Pavel Marek, born 1932, obtained his civil engineering degree and PhD at the Czech Technical University in Prague. Over the past 25 years, he has been involved in structural steel research and teaching at Czech and foreign universities. At present, he is a Visiting Professor at the San Jose State University of California.

Milos VLK
Assoc. Prof.
Technical University
Brno, Czechoslovakia

Pavel Vlk, born 1937, received his mechanical engineering degree at the Technical University in Brno. For 23 years, he studied fatigue and brittle fracture and applications of findings to industrial practice. At present, he is a university teacher.

Ivo HEPNAREK
Dr. Eng.
Vitkovice-Institute of Applied Mechanics
Brno, Czechoslovakia

Ivo Hepnarek, born 1948, received his civil engineering degree at the Technical University in Brno. Fields of professional interest are numerical and experimental analysis of static and dynamic response of full-scale steel structures.

SUMMARY
This paper presents a method of recording and evaluating the accumulation of fatigue damage using an electronic device. User needs and available evaluation algorithms are discussed. The paper also includes a brief description of the hardware and software aspects. Finally, experience from field use, an example and future prospects are presented.

RÉSUMÉ
Cet article présente une méthode d'enregistrement et d'analyse du dommage de fatigue faisant intervenir un dispositif électronique. Les besoins de l'utilisateur ainsi que les algorithmes d'analyse à disposition y sont discutés. L'article contient également une brève présentation de quelques aspects du matériel et du logiciel. Enfin, il présente des expériences d'applications pratiques, un exemple ainsi que des développements futurs.

ZUSAMMENFASSUNG
Der vorliegende Artikel erläutert eine Methode zur Aufzeichnung und Auswertung der Schadensakkumulation infolge Ermüdung mit elektronischen Hilfsmitteln. Bedürfnisse der Benützer sowie zur Verfügung stehende Auswertungs-Algorithmen werden diskutiert. Ebenso ist eine kurze Beschreibung einiger Hard- und Softwareaspekte enthalten. Erfahrungen aus praktischen Anwendungen, ein Beispiel und künftige Entwicklungsmöglichkeiten werden vorgestellt.

1. INTRODUCTION

In using the Limit States Design Method for assessment of reliability, the structure and its components are considered to have adequate reliability if the defined most unfavourable responses, the extreme characteristics, do not exceed the limit value. These values, defined for all the reliability conditions during the life of the structure, can be grouped in carrying capacity limit states and serviceability limit states.

Special attention has to be paid to the evolution of the extreme characteristics of the structure to the loading. Especially in case of fatigue and for the evaluation of the accumulation of fatigue damage during the lifetime lack of input data may cause severe problems.

The subject of this paper is a description of a device which allows recording of the time dependent response of a structure to the loading and easy evaluation of the accumulation of fatigue damage as well as corresponding residual fatigue life.

As electronic components become more reliable and consume less power so that a device can be operated for long periods of time without maintenance, an idea has emerged to build a device which can replace costly and sensitive apparatuses like tape recorders to collect, preprocess and store information on the response history of metallic structures such as bridges, guyed masts etc. It was clear in the very beginning that such a device has to be designed to withstand various climatic and mechanical stresses. For that purpose, one-chip microcontrollers and other integrated circuits are an ideal solution.

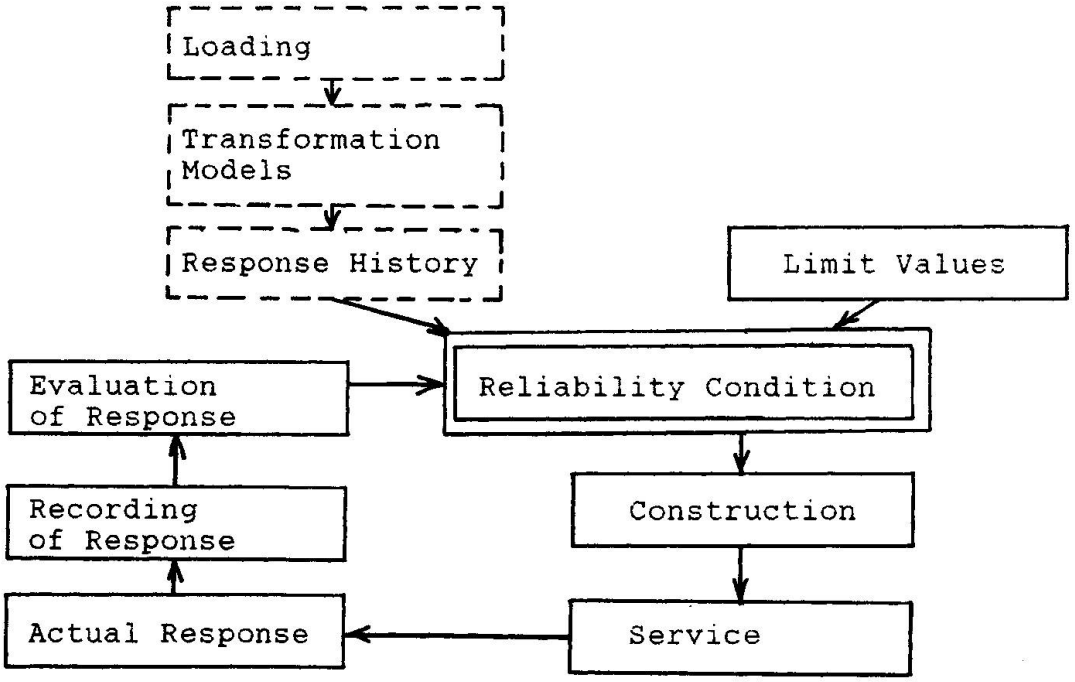

Fig. 1 Feedback Loop

2. USERS' DEMANDS ON THE DEVICE

In order to make the purpose of the device clear, let be mentioned the case when there are substantial uncertainties in the loading and/or the transformation model to establish the response to the loads as discussed in the feedback loop (see Fig. 1).

The structure is built and assessed subsequently based on observations in service. The response history is then evaluated and used as feedback to assess the reliability conditions. This approach is used quite frequently in the assessment of the reliability condition for fatigue [2]. It may lead to a modification of the existing structure or to an increase in the general body of knowledge, improvement of specification, etc.

The purpose of the device is the monitoring of the strain history of the metallic structure and recording the processed information in a non-volatile memory. The operator then connects the communication cable with the device and transfers the stored data into a portable computer where the information is to be evaluated.

This formulation was precised during the developing of the device, in connection with obtaining more information on the recording device currently used by the customer, while the compatibility became the main point of view, for example, analog input within the range of +- 12 V of the measured quantity was required.

There were several demands on the ease of operation and maintenance and flexibility. In the lab sample, six channels of analog input were implemented and active channels are selected by the software. Two methods of the preprocessing of the information and input hystheresis were to be selectable. For verifying the design, switches were used in the device, but in production the options will be firmware-selected so that less reliable components and cables can be eliminated.

The information is to be stored in a non-volatile memory. A CMOS memory device, backed-up by a battery, was used to satisfy the demand. The capacity of the memory can range between 2K and 16K bytes, depending on the method used and the number of channels.

Two methods of transferring the data into some evaluating device have been considered. The first possibility is to use a standard serial communication cable and to transfer the data in the desired format (RS 232) into a computer carried by the operator. An IBM PC compatible or the Sharp portable computer are two examples.

The second method is to replace the whole memory module by a fresh one and to carry the recorded module to the office where its contents can be read by a special adapter connected to a personal computer. This method eliminates the need of the computer to be carried into the field.

3. THE HARDWARE SOLUTION

The hardware has been designed to use Czechoslovak components where possible. An 8048 microcontroller with an external program memory has been chosen for the lab sample in order to achieve a greater debugging ability. For volume production, the 8748 or 80C48 types with a built-in program memory and a low power consumption are to be used.

The controller is clocked by a 6 MHz oscillator from which the timing information is derived to the timer and the baud rate generator. The controller's bus and ports communicate with the program storage, analog multiplexer, A/D converter, serial port, configuration switches and 8255 peripheral circuit to which the memory module is attached.

The analog input circuitry is designed to process up to six input signals within the range from -12V to +12V. The range is divided into 256 levels.

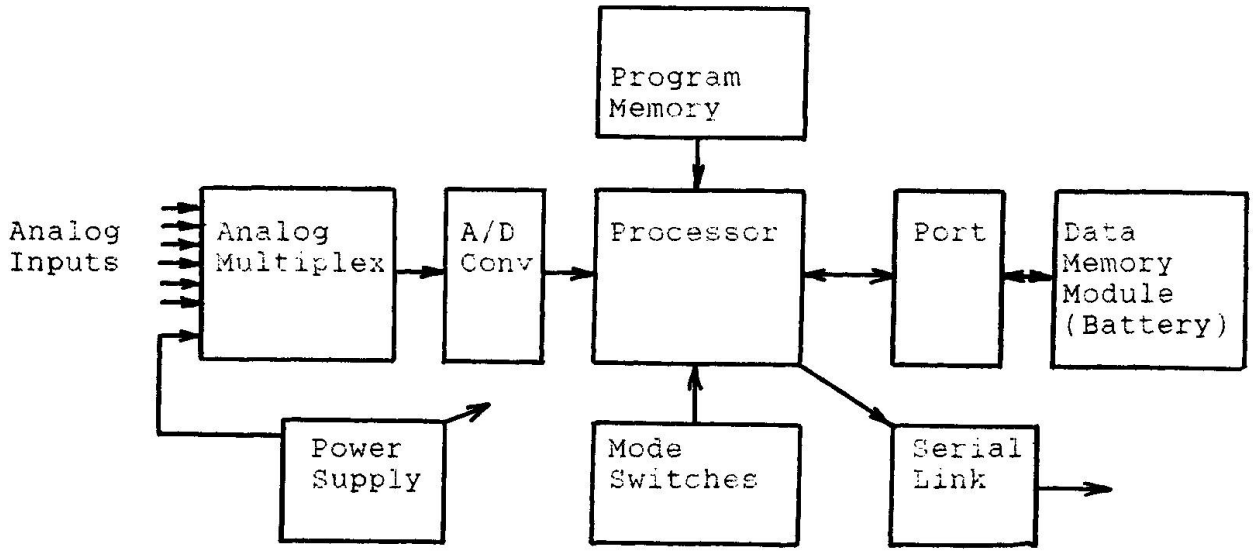

Fig.2 Block diagram of the device

The input analog multiplexer connects one of the six inputs to the A/D converter. Another analog signal can be selected by the multiplexer: the power sense signal which indicates the power failure. In that case the microcontroller disables the access to the memory.

The A/D converter converts the value of the input voltage to an 8-bit number. Though a lower resolution is required by the software, this amount of information is easy to manipulate with and is used for generating the input hystheresis. The binary number is obtained by a software controlled D/A converter and a comparator.

The asynchronous serial port is also software driven by one bit of the microcontroller's port. The TTL level signal is transformed to RS 232 levels. The transfer rate is software selectable; in the lab version 2400 bps are selected.

The configuration switches select the options of operation:

active channels, hystheresis and the preprocessing method.

An 8255 programmable peripheral interface is used to control the non-volatile memory in which the preprocessed information is stored. The memory is not directly connected to the microcontroller so that the memory module can be easily removed from the device and replaced by a fresh one. The 8255 circuit generates the addresses and control signals for the memory, the data are transferred through one of its ports. The memory cycles are controlled by the software. In the beginning of each cycle, supply voltage is checked so that in the case of a power failure the data can not be damaged. After the data are written into the memory, the checksum in the last byte is updated to ensure the data validity. If a power failure occurs, the controller notices it and resets the 8255 circuit whose ports go to the low level. Thus, the content of the memory is kept intact because the memory access is initiated by a high level on the module's control inputs.

The memory module itself consists of one or two CMOS memory circuits and CMOS logic circuits, a battery and other elements. The CMOS devices are permanently powered by a lithium battery on-board. The battery life can be estimated at five years.

During the transportation of the memory module, its inputs are kept low by resistors. In the reading adapter in the office the module is repowered by an external source and its content can be read and written into.

The power source for the device can be selected to be supplied by several voltages. In the lab sample, a simple 220 Vac 50 Hz line was chosen. Under certain conditions, when operated in a mobile structure, a 24 Vac supply may be preferred as well as a dc-dc transducer.

The device, when operated in extreme low temperature conditions like in a mountain area, may contain a thermostatic subsystem that keeps its temperature within the allowed range. The system's tolerance to high temperatures is determined by the quality of the used components and can be estimated at 100 deg C. The heat production of the device itself is very low due to the low-power CMOS technology used.

The lab sample was designed to verify the function and explore the possibilities and the users' real needs; that is the reason why its mechanical construction was not the main imperative point of view. However, the planned volume-production devices should withstand raw mechanical conditions. This aim will be achieved by using the quality printed circuit board technology with as small moving parts as possible, reliable components and a robust metallic case.

4. SOFTWARE

The software has been written in the microcontroller's machine language so that the demands on optimal code are fulfilled. The microcontroller's internal memory is very limited and it cannot be saved during power failure. Thus, the data memory must always keep all information needed.

The software in the program memory has three main parts. The first part is used for interfacing with the 'real world'. It manages the input signal selector, the A/D conversion, the power check and the timer.

The second part is the data preprocessing and storing into the memory. It is dependent on the employed method of analysis; the rain-flow method was used in the lab sample, the options using or omitting the mean value are selectable. This part also manages the memory depending of the number of inputs and the method used.

The third part was incorporated into the program for outputting the data via the serial line. This part gets the data from the memory, converts them to a convenient ASCII format and transmits them through the port using its own baud rate generator.

5. FIELD USE

The experiments verified the device's ability to collect the information from one of several analog sources, preprocess it using the rain-flow algorithm, store the data in the non-volatile memory and output them to the operator. There is a connection of the maximum number of channels, computing the requirements of the method used, the processor's speed and the input bandwidth, and also a connection between the storage demands of method used, the number of channels and the required capacity of the data memory.

The field usage confirmed the need of a reliable operation because one unreliable connector can cause a loss of worthy data.

6. EXAMPLE

As an example, applying the device in evaluating the lifetime of excavator for the brown coal surface mining may be mentioned. The stress in the evaluated location was measured in a selected operating mode in the coarse of approximately one month. The obtained representative spectrum of the response is shown in Fig. 3. This information was further used in estimating the life to initiation of fatigue crack.

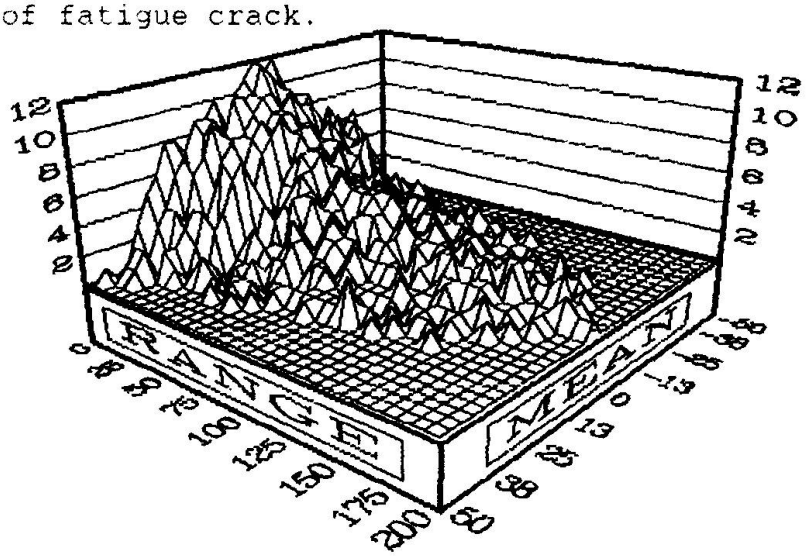

Fig. 3 An example of evaluated data

7. CONCLUSION AND FUTURE PROSPECTS

This paper described a method of measuring, processing and storing the data on fatigue damage of the structure. A microprocessor-based electronic device doing that job was presented. We hope that in mass use, thanks to its low price, it may be mounted permanently on critical parts of the structure and monitor its history so that the residual life may be determined as well as theoretical knowledge may be acquired.

The device should collect and evaluate the data concerning the level of the fatigue damage in real time and accumulate it for long periods of time.

References

[1] Marek, P. - Kennedy, D. J. L.: Development of Structural Steel Design Standards. University of Alberta, Dept. of Civil Eng., Structural Eng. Report 154, October 1987, Edmonton.

[2] Dibley, J.E. - Wilson, A. B. - Bose, B.: Fatigue Monitoring on an Ore Unloader. In: Proceedings of IABSE Colloquium "Fatigue of Steel And Concrete Structures", Lausanne 1982.

Leere Seite
Blank page
Page vide

Vibration Fatigue of Steel Bridges of the Bullet Train System

Fatigue due aux vibrations dans des ponts en acier du réseau de trains à grande vitesse

Schwingungsbedingte Ermüdung von Stahlbrücken des Japanischen Schnellzugnetzes

Kenji SAKAMOTO
Chief Researcher
Track & Structure Laboratory
Tokyo, Japan

Chitoshi MIKI
Associate Professor
Tokyo Inst. of Technology
Tokyo, Japan

Atushi ICHIKAWA
Chief Researcher
Track & Structure Laboratory
Tokyo, Japan

Makoto ABE
Researcher
Track & Structure Laboratory
Tokyo, Japan

SUMMARY
Fatigue cracks caused by out-of-plane vibration were observed in steel bridges of the Tokaido Shinkansen. Crack growth behaviour, measured cyclic stresses, evaluation of fatigue damage, and retrofitting methods are described.

RÉSUMÉ
Des fissures de fatigue causées par des phénomènes de vibration dans les éléments ont été observées sur des ponts en acier du Tokaido Shinkansen. Cet article présente le comportement de la propagation de ces fissures, les mesures des cycles de contraintes, l'évaluation du dommage en fatigue, ainsi que les méthodes de réparation possibles.

ZUSAMMENFASSUNG
In Stahlbrücken der Tokaido Shinkansen-Expresslinien wurden Ermüdungsrisse festgestellt, die vermutlich durch Schwingungen einzelner Elemente aus ihrer Ebene verursacht wurden. In diesem Bericht werden das Ausbreitungsverhalten solcher Risse, Messungen zyklischer Belastungen, die Ermittlung des Ausmasses von Ermüdungsschäden sowie mögliche Instandstellungsverfahren erläutert.

1. INTRODUCTION

One quarter century has passed since the Tokaido Shinkansen was opened for service. Tokaido Shinkansen is one of the bullet train system in Japan operating at the maximum speed of 220km per hour 230 trains daily (Fig.1). Various types of fatigue damages have happened in steel bridges of Tokaido Shinkansen, some of them being comparatively rare with the those in bridges of conventional railway system. Fatigue crackings due to the out-of-plane vibration-induced stresses are typical ones which appeared in the plate girder bridges, box girder bridges and stringers of truss bridges. Vibration-induced stresses under the passage of bullet trains at these bridge details are not of very high amplitude, but of high frequency. No fatal accident due to this type of crack has yet been reported, but retrofitting works are essential to meet the recent demand for an increasing train speed of 270km per hour and a greater transportation capacity. This report describes a behaviors of fatigue cracking, stress measurements, retrofitting works applied and results of remaining life evaluation.

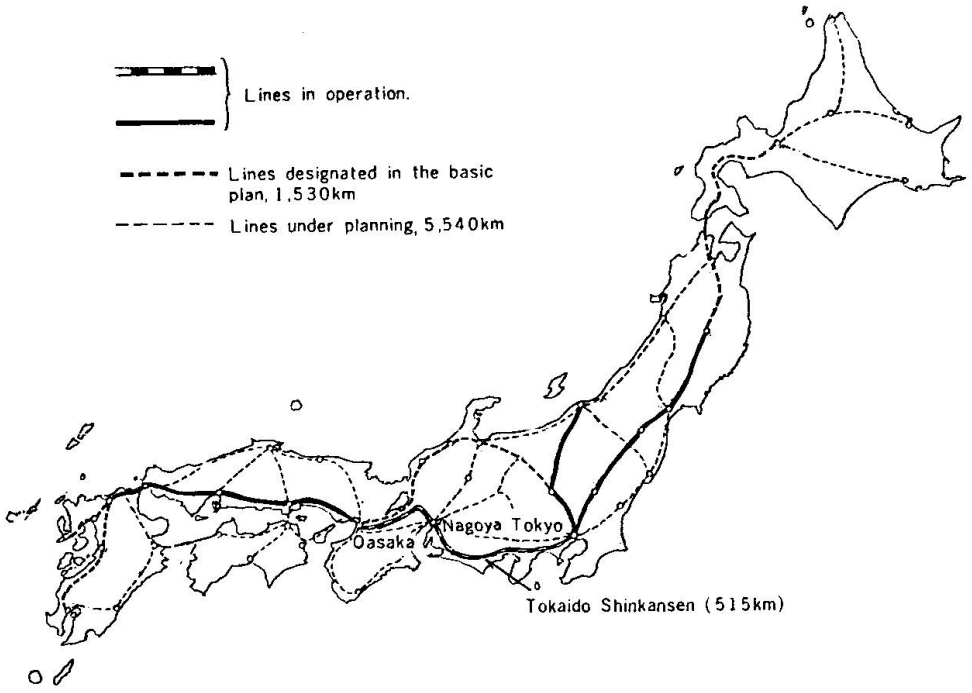

Fig.1 Network of bullet train system

2. OUTLINE OF THE BRIDGE STRUCTURE OF THE TOKAIDO SHINKANSEN

Table 1 shows the quantities of bridges by type of the Tokaido Shinkansen. Steel bridges were designed in accordance with the design specifications established in 1961 and welded structures were adopted for all shop joints. Fig.2 shows the design live load and anticipated use conditions of the Tokaido Shinkansen.

Type	Structure	Number of spans
Steel	Deck plate Girder (I section)	194
	Box Girder	139
	Through plate Girder	155
	Composite Beam	258
	Through Truss	135
Concrete	Reinforce Concrete	3307
	Presstrest Concrete	389
Total		4577

Table 1 Quantities by Bridge Type

Anticipated use conditions

Maximum speed	200 km/h
Number of trains per day	80
Number of cars per train	8 or 12
Design fatigue life	70 years

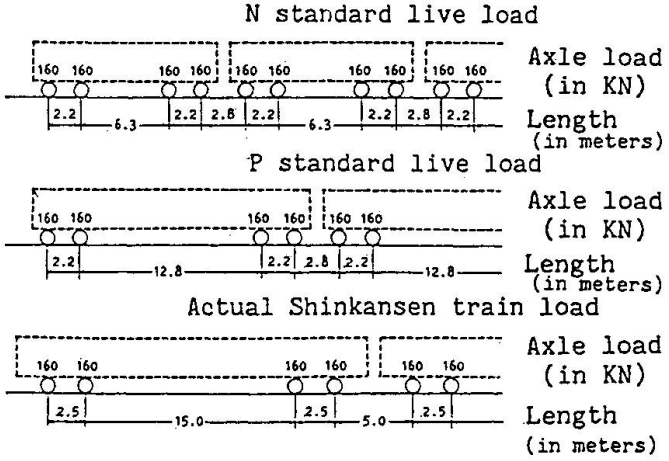

Fig.2 Design live load and anticipated use conditions

Table 2 shows allowable fatigue stresses for various types of joints in the 1961 specifications. These allowable fatigue stresses were based on the fatigue strength at 2 x 10^6 cycles of each structural joints. The designer used the load of 180 kN axle weight which are 20 kN larger than the axial load of the design load as shown in fig.2, taking into consideration a possible increase in traffic in the future. By the end of December 1989, nearly one million trains had passed along the line. The steel bridges in the Tokaido Shinkansen have suffered very severe loading condition caused by high-speed train operation and highly repetitive frequencies. Nevertheless, a fault in the structure has never led to an accident.

In the process of their service, however, some types of fatigue damage have been observed as shown in fig.3. No fatigue damage due to low fatigue strength has not observed in main members where fatigue was assessed in the design stage. However, fatigue cracks which are the result of secondary stresses and displacement induced stresses are often discovered in such various structural elements as girder webs, stringer webs, floor beam webs, side walks, connections of attached facilities and diaphragms. One of these fatigue crackings which occurs relatively frequently and whose cause has not been made much clear is a fatigue crack which occurs on a web plate at the lower end of a siffener (hereinafter referred to as the "lower end of a stiffener"). This fatigue cracks is in parallel with the lower flange.

Category	Types of stress	Fatigue allowable stress (kg/cm²)	Types of joints
A	Tension	$\frac{2000}{1-2/3k}$	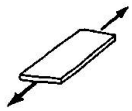
$\bar{A}$	Compression	$\frac{2400}{1-k}$	
B	Tension	$\frac{1500}{1-2/3k}$	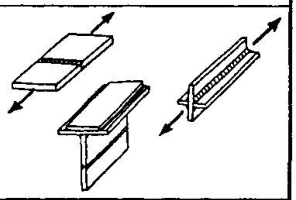
$\bar{B}$	Compression	$\frac{1800}{1-k}$	
C	Tension	$\frac{1260}{1-3/4k}$	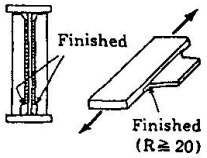
$\bar{C}$	Compression	$\frac{1440}{1-k}$	
D	Tension	$\frac{1000}{1-2/3k}$	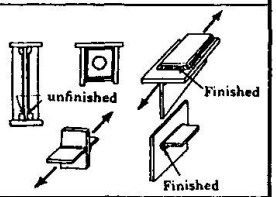
$\bar{D}$	Compression	$\frac{1200}{1-k}$	
E	Tension	$\frac{700}{1-3/4k}$	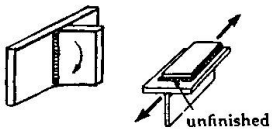
$\bar{E}$	Compression	$\frac{800}{1-k}$	

Note, $k = \frac{|\sigma|_{min}}{|\sigma|_{max}}$

Table 2 Fatigue allowable stress (1961)

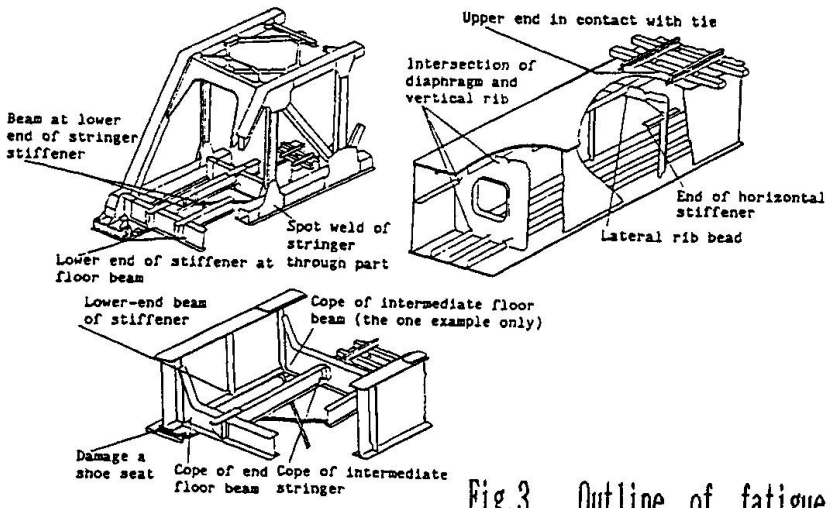

Fig.3 Outline of fatigue damage

3. VIBRATION INDUCED FATIGUE CRACKS IN THE LOWER END OF THE STIFFENER

Fig. 4 shows cracked girder web. This type of fatigue cracks occurred at the lower end of the stiffener on girder webs of box girder bridges and stringer webs of through truss bridges. Characteristically, no crack has occurred at the end of the stiffener to which floor beams or sway bracings are connected. These fatigue cracks began to be observed in 1978. To date, cracks have been observed in about 10,000 details of about 200 box girder bridges and in about 100 details of five through type truss bridges. Countermeasures were taken against all parts of through type truss bridges which were considered to undergo cracking.

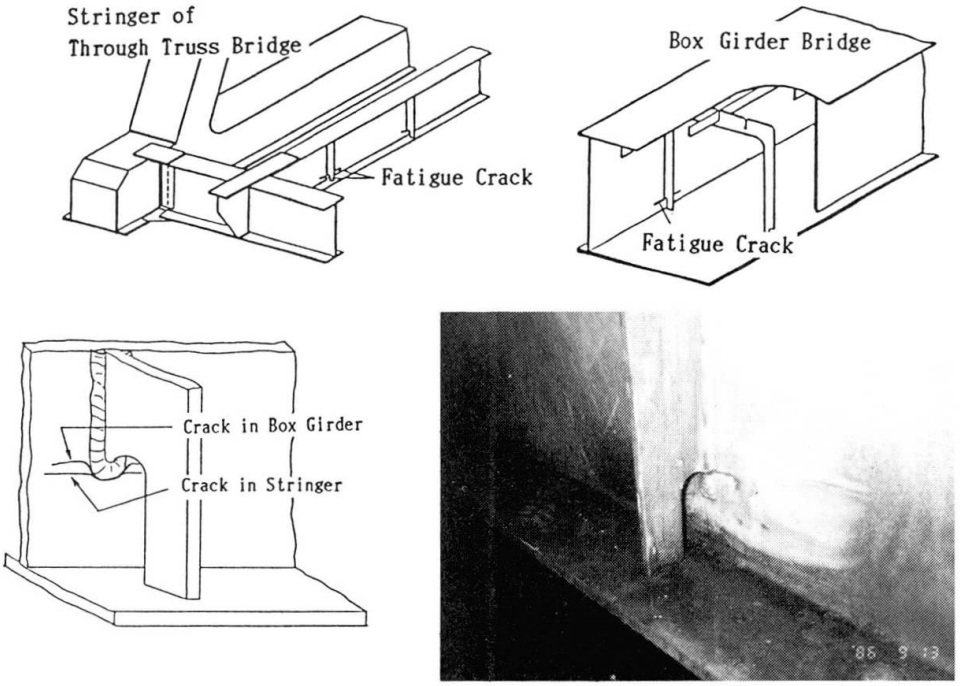

Fig.4 Fatigue crack at stiffener end

4. FAILURE MODE AND ANALYSIS

4.1 Measurement of the Cyclic Stresses

The stringer of a truss bridge was selected for cyclic stress study. This truss bridges has a standard floor system of the Tokaido Shinkansen whose span is 60 m, and the span of stringers is about 10 m. Measurement was made by comparison concerning whether there are sway bracings(Fig.5) and differences in train speeds. Dynamic strain measurement was conducted by placing strain gauges to the back and surface of the web plate at the lower end of the welded portion. The strain gauges were located 5 to 10 mm away from the lower end of weld toes (Fig. 6) stress records were processed as follows.

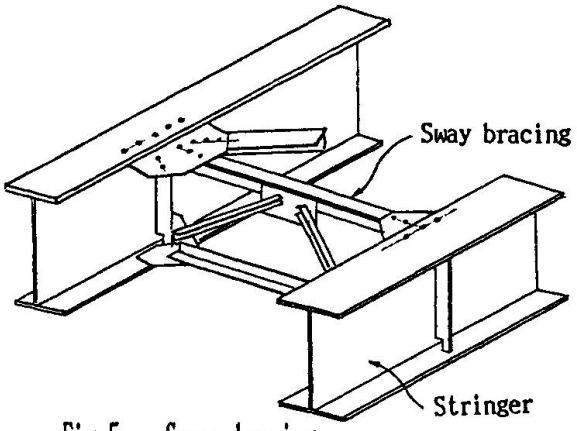

Fig.5 Sway bracing

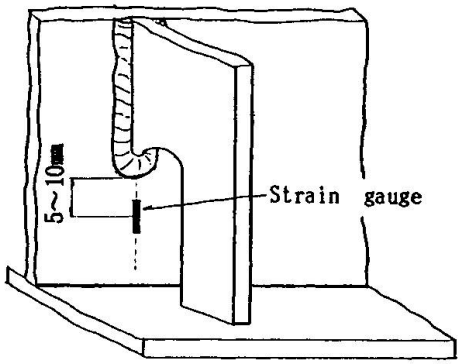

Fig.6 Position of strain gauge

(1) Stress-time analog records were transformed into digital data and the range pair method was applied to obtain stress range histgram.

(2) The linear damage law (modified Miner's law) was applied to evaluate the degree of fatigue damage. The JNR category B design curve was used in the analysis because measured stresses include some influence of stress concentration due to weld beads.

4.2 Results of Measurements and Analysis

Fig.7 shows a typical stress records on the stringer web and the results of frequency analysis. S-1 and S-2 are stress records at same point of stiffener end detail without sway bracing when a train passed away at a speed of 203 km/h and 178 km/h respectively. S-3 is a stress by train passing at a speed of 203 km/h at a position to which sway bracing is connected. Train speeds were obtained, using a strain gauge fitted to the track. Major results of this test can be summarized as follows;
As obviously shown by the comparison between S-1 and S-3, at the detail where sway bracing exists, stress amplitude is smaller than where sway bracing does not exists, and the high-frequency component is also smaller. This is considered to be due to horizontal vibrations of the lower flange.
Stresses in S-1 is the largest measured value in this structure and its stress waveform exhibits a resonating behavior. However, S-2, the stress waveform of a low-speed train (v=178 km/h) does not produce as large stress as S-1 (v=203 km/h). Therefore, horizontal vibration of the lower flange was induced only by the passage of high speed trains. In order to examine this resonating behavior, a stress was separated into the in-plane component and the out-of-plane component as shown in Fig.8. Its results indicate that the stress at the lower end of the stiffener without sway bracing detail is mainly caused by out-of-plane distorsion of the web plate. From this, it seems possible to say that the source of a predominating stress which occurs at the lower end of a stiffener is horizontal vibrations of the lower flange.
Fig.9 shows the stress histgram and the degree of fatigue damage of each stress component. The results suggest that fatigue cracks occurred in several years under S-1 stress history.
However, S-2 shows not so high degree of damage.

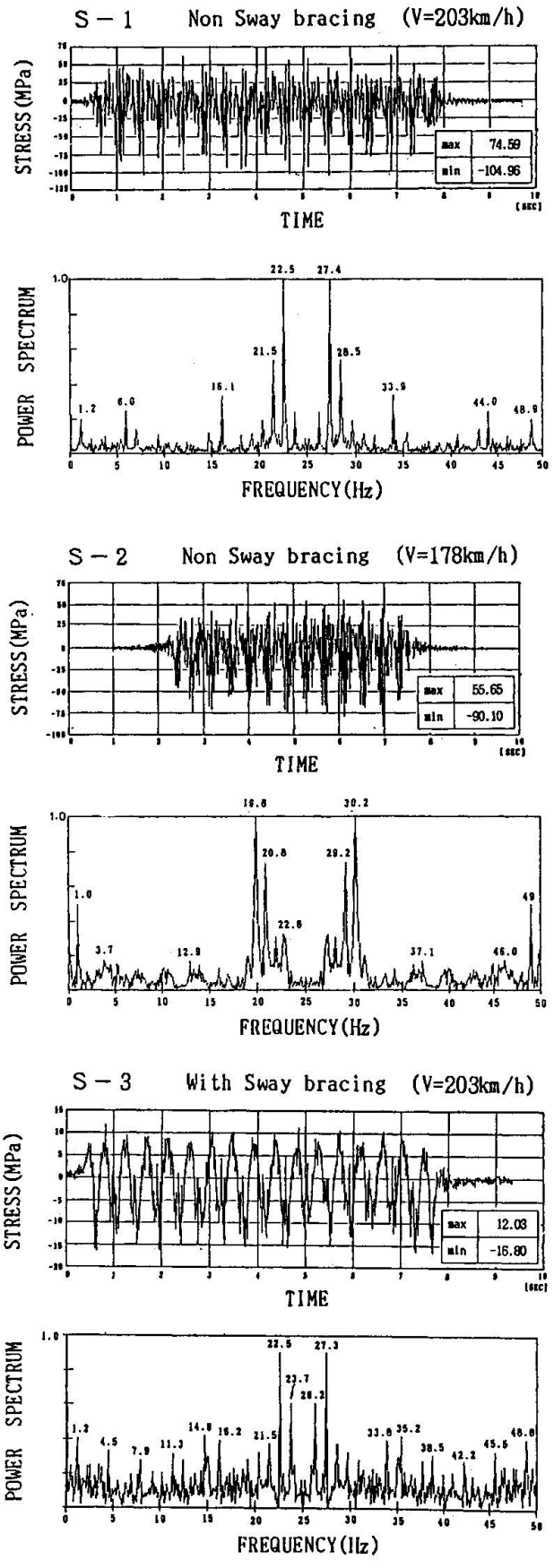

Fig. 7 Representative stress wave in Bridges mesured

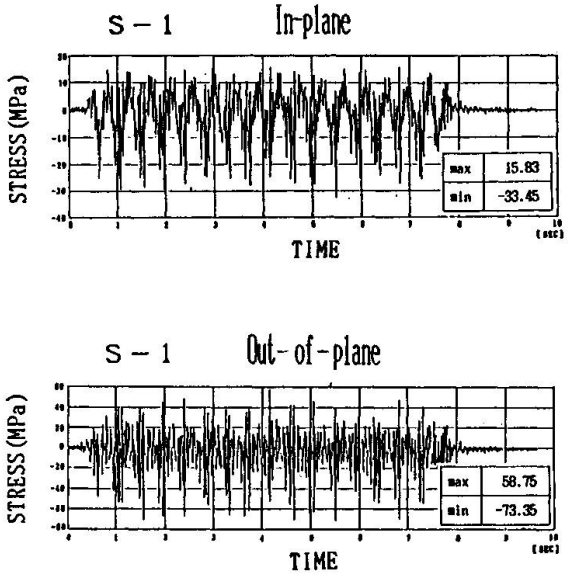

Fig.8 Stress component in In-plane and Out-of-plane of web

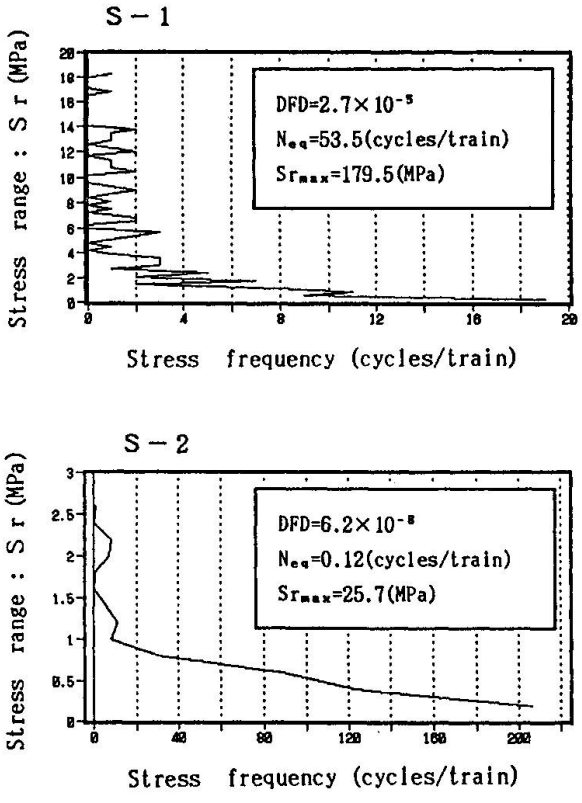

Fig.9 Stress frequency and Degree of Fatigue damage (DFD)

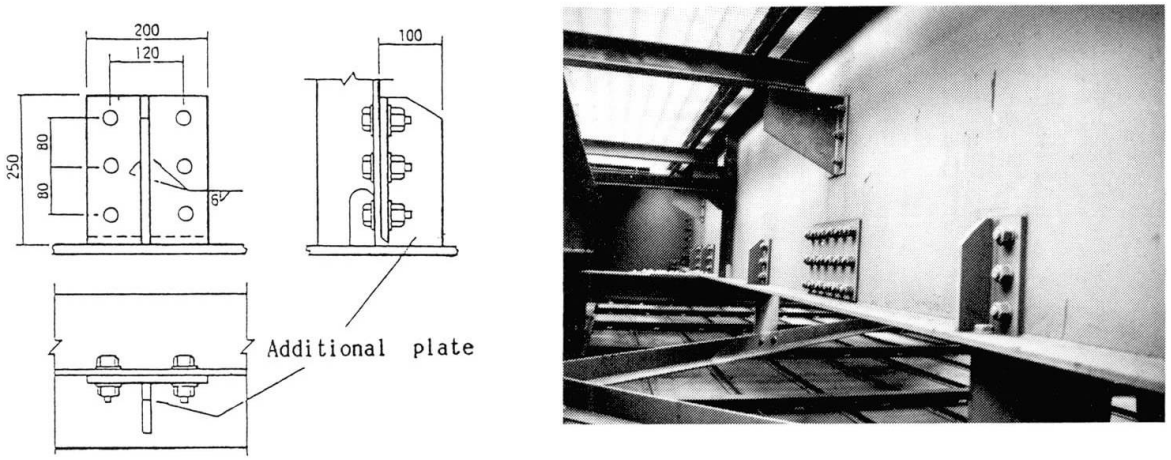

Fig.10 Retrofitting by additional plate

5. RETROFITTING METHODS

As a countermeasure against these fatigue cracks, it is most effective to stop local horizontal vibrations of lower flange which cause fatigue cracks. In some truss bridge stringers, fatigue cracks were removed by applying of arc air gouging and rewelded and then an additional plates were installed by high-strength bolts (Fig. 10). In some cases a sway bracing was also added. Another possible measure is to increase the fatigue strength of the detail. As it is costly to add plates to a slight fatigue crack, it was necessary to consider an economic method for raising fatigue strength. It is advisable to improve the fatigue strength of the toe of a fillet weld and prevent occurrence of additional crack in a part where occurrence of a fatigue crack is not confirmed as a preventive measure. Application of TIG (Tungsten Inert Gas) arc remelting has considered as an effective and economic method for repairing a fatigue crack at the toe of a fillet weld and improving fatigue strength.

5.1 Application Test of TIG Arc Remelting

Repair of the Lower end of a stiffener by TIG arc remelting is required to be conducted, while ensuring that the form of the toe of a fillet weld will be smooth and that penetration will be deep enough to fuse slight fatigue cracks which occur at the toe and is visually undiscoverable. The appearance of the bead under various application conditions and the amount of fusion in the boxing-welded portion were investigated. As a result, it was found that under the conditions as shown in Table 3 fusion was about 2mm in the case of stand-up position and the shape of the bead was in good condition. It was also found that confirmation of the position of a crack is necessary in carrying out the work because there is the possibility of a gap occurring between the position of the maximum fusion by the TIG dressing and the position of a crack.

Electrode diameter	3. 2㎜
Current	240A
Voltage	13～14V (arc length 0～1㎜)
Speed	45～60s/100㎜
Aiming position	0 to 1㎜ from the toe of weld
Torch angle	90°

Table 3 Condition of TIG arc remelting

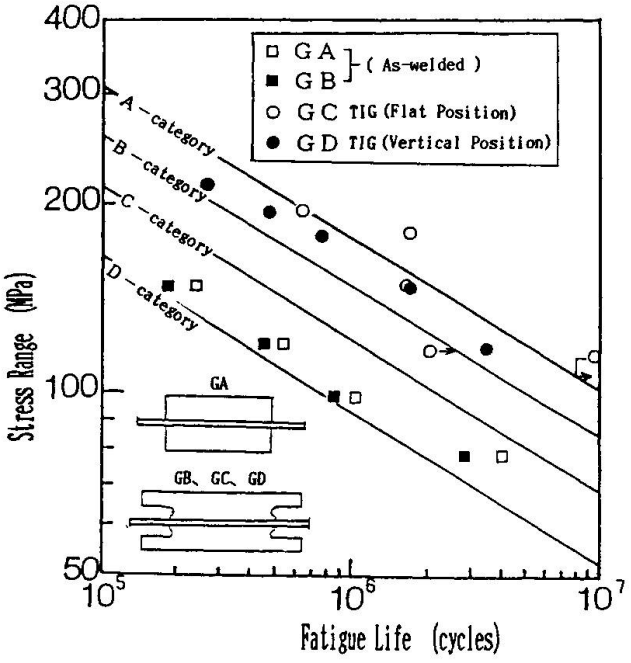

Fig.11 Results of fatigue test

5.2 Improvement of Fatigue Strength by TIG Dressing

In order to confirm the effect of the TIG dressing on this stiffener end detail, fatigue testing was conducted on specimens simulating this detail and applying conditions in actual bridges. Two type of specimens(GC and GD) were TIG dressed under the conditions as given in Table 3. Specimens GC were treated by TIG arc remelting in a face-down position and specimens GD were TIG dressed in a stand-up position, considering actual application conditions.
The result of fatigue testing is shown in Fig. 11. It was found that the fatigue strength of as-welded specimens slightly exceeded the category D of the design curve, while the fatigue strength of TIG dressed specimens exceeded the category B curve. The TIG dressing improved the shape of the toe of weld which affects occurrence of a crack and reduces stress concentration, thus improving fatigue strength.

6. OTHER CONSIDERATION IN FIELD APPLICATIONS OF TIG DRESSING

In executing the work, it was decided that the working procedure would be established as given in Fig.12. All details were observed by qualified inspectors by using eddy current test and magnetic particle test. Before applying the TIG dressing, the shapes of beads were examined. As a result, no special problem was found in the appearance of the beads. However, due to excessive grinding of beads at the time of manufacturing, throat depths of fillet welds were found to be unsatisfactory in some details. In such a weld, in addition to the countermeasures as given in 5, a measure to prevent occurrence of a fatigue crack from the root is necessary. One or two passes of fillet welds were added to such details.

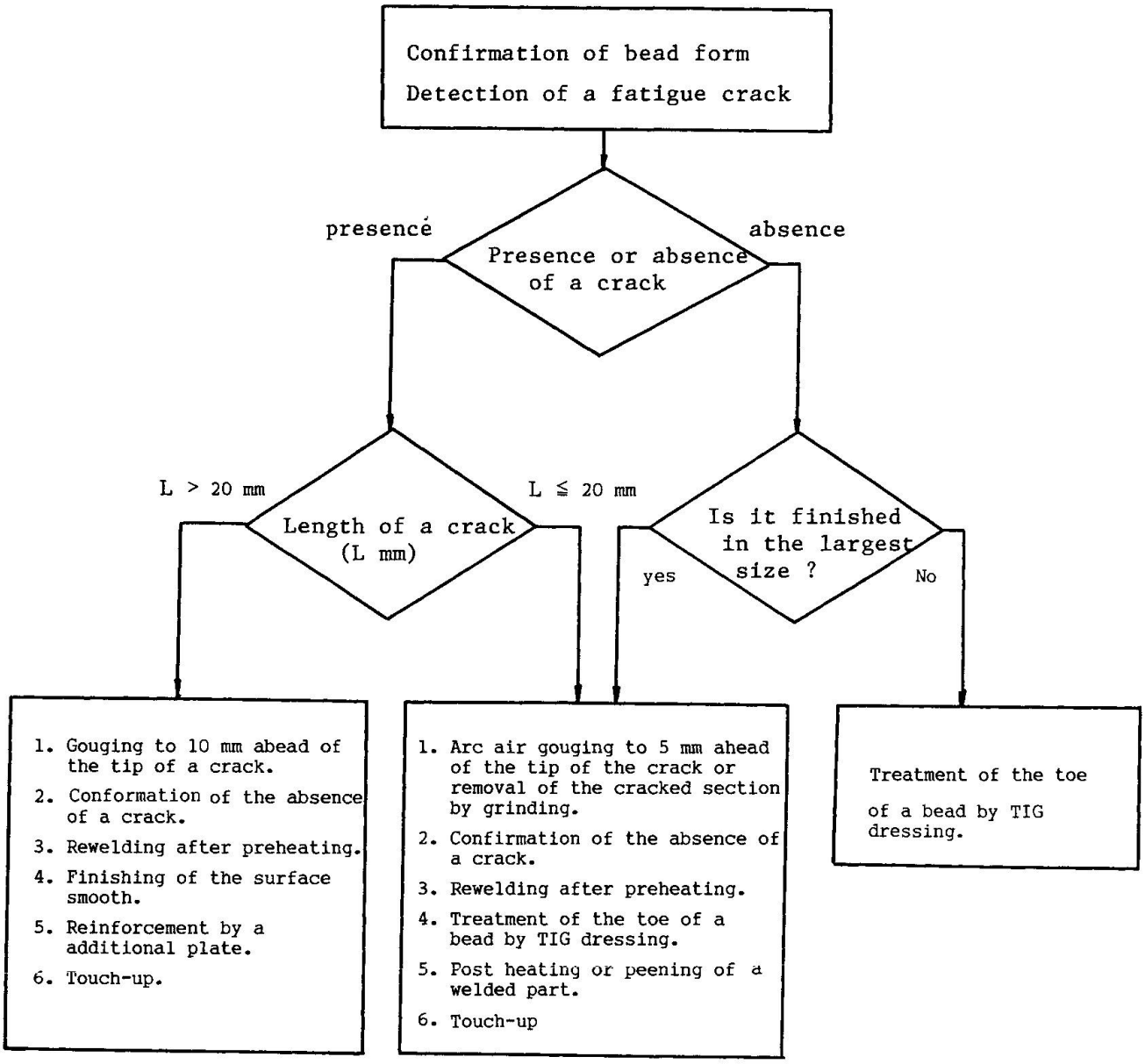

Fig. 12 Retrofitting process

7. CONCLUSION

The retrofitting by the TIG dressing was conducted in 300 box girders. The repaired parts have been inspected specially emphatically but recurrence of a fatigue crack has not been reported.
At present, an evaluation of current soundness is underway for all steel bridges of the Tokaido Shinkansen in preparation for higher speeds and larger transport capacities in the future. As part of this program, several bridges of all types were selected as model bridges and various studies including local stresses, fatigue crack growth behavior in various structural details, and monitoring system of fatigue cracking are being performed.

Fatigue of Cross-Beam Connections in Plate-Girder Highway Bridges

Fatigue dans les attaches des entretoises de ponts-routes à section ouverte

Ermüdung der Querträger-Anschlüsse in Strassenbrücken mit offenen Querschnitten

Ichiro OKURA
Assist. Prof. of Civil Eng.
Osaka University
Osaka, Japan

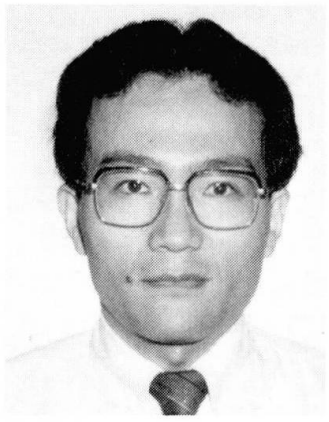

Ichiro Okura, born 1955, received bis BSc, MSc und Dr. Eng. degrees in civil engineering from Osaka University in 1977, 1979 and 1985, respectively. His research field is steel structures.

Yuhshi FUKUMOTO
Prof. of Civil Eng.
Osaka University
Osaka, Japan

Yuhshi Fukumoto, born 1932, received his MSc degree in civil engineering from Kyoto University and PhD degree from Lehigh University. He has held professorship at Nagoya University from 1963 to 1986.

SUMMARY

Fatigue cracks often grow from connections of cross beams to main girders in plate-girder highway bridges. The structural parameters which govern cracking at cross-beam connections are examined based on the overall behaviour of the bridges. Cracking patterns at cross-beam connections are determined from fatigue tests. A recommendation is given for connection details between concrete slabs and main girder flanges.

RÉSUMÉ

Les fissures de fatigue prennent souvent naissance à la liaison entre les entretoises et les poutres maîtresses des ponts-routes à section ouverte. Les paramètres structuraux qui régissent la fissuration aux liaisons avec les entretoises sont examinés en se basant sur le comportement global des ponts. Des modèles de fissuration des liaisons avec les entretoises sont déterminés à partir d'essais de fatigue. Une recommandation est donnée pour des détails de liaison entre la dalle de béton et les ailes des poutres maîtresses.

ZUSAMMENFASSUNG

Ermüdungsrisse in Strassenbrücken mit offenen Querschnitten gehen oft von den Verbindungen zwischen Quer- und Hauptträgern aus. Die Einflussfaktoren, die den Rissverlauf an den Verbindungsstellen bestimmen, werden unter Berücksichtigung des Gesamtverhaltens der Brücke untersucht. Das Rissverhalten an den Verbindungsstellen wird anhand von Ermüdungsversuchen betrachtet. Es werden Empfehlungen gemacht zur Gestaltung der Konstruktionsdetails bei der Verbindung zwischen Betonfahrbahnplatte und Hauptträgerflansch.

1. INTRODUCTION

In many plate girder highway bridges in the urban area of Japan, fatigue cracks are often observed at the connections of main girders with secondary members such as cross beams, sway bracings and lateral bracings. At the connections of cross beams to main girders in the plate girder bridges of the Hanshin Expressway in Osaka, four types of fatigue cracks are detected, as shown in Fig.1.

-Type 1 crack is initiated either on the bead or at the toe at the end of the fillet weld between the connection plate and the top flange of the main girder.
-Type 2 crack is initiated at the upper scallop of the connection plate, and grows diagonally through the connection plate itself.
-Type 3 crack is initiated at the toe at the end of the fillet weld connecting the connection plate to the main girder web, and grows downward along the toe on the connection plate side.
-Type 4 crack is initiated and grows along the toe on the web side of the fillet weld between the top flange and the web of the main girder.

Investigation of the causes of the crack initiation and the development of repair methods have been under way at various research institutions. However satisfactory results are not yet available.

In 1985 the authors carried out the field stress measurement of an existing plate girder bridge of the Hanshin Expressway to make clear the local stresses causing the cracking at the cross-beam connections[1,2]. They then formulated the relationship between the local stresses and the three-dimensional behavior of the bridge under traffic loading[3].

The objectives of this paper are:

-to present the parameters introduced from the structural behavior of a plate girder bridge, which govern the cracking at the cross-beam connections,
-to show the patterns of the cracking at the cross-beam connections from fatigue tests, and
-to give a recommendation to the connection details between concrete slab and main girder flange.

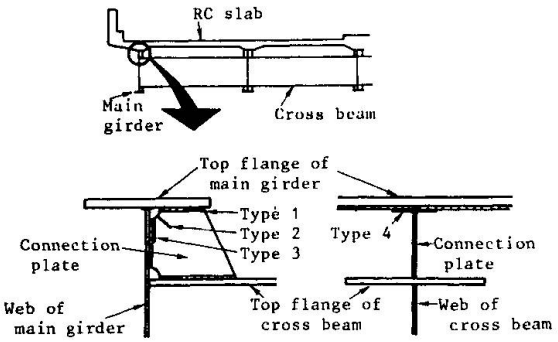

Fig.1 Fatigue cracks at cross-beam connections of plate girder bridge

2. STRUCTURAL PARAMETERS AFFECTING CRACK INITIATION

2.1 Relationship between Local Stresses and Rotations of Concrete Slab and of Cross Beam

As shown in Fig.2, the membrane stress σ_{my} in the vertical direction in the connection plate and the plate-bending stress σ_{by} in the main girder web are main factors to cause Types 1 and 4 fatigue cracks, respectively[1,2]. The relationship between those local stresses and the rotations of concrete slab and of cross beam is given by[3]

$$\begin{bmatrix}\sigma_{my}\\ \sigma_{by}\end{bmatrix} = \begin{bmatrix}k_{m1} & k_{m3}(\gamma-k_{m123})\\ k_{b1} & k_{b3}(\gamma-k_{b123})\end{bmatrix}\begin{bmatrix}\theta_{s0}\\ \theta_{g}\end{bmatrix} \tag{1}$$

where θ_{s0}=rotation of concrete slab due to the slab-deformation caused by wheel loads(see Fig.3), θ_g=rotation of cross beam due to the vertical displacements of main girders(see Fig.3), γ=coefficient depending on the position of a vehicle in the direction of the roadway width, and k_{m1}, k_{m3}, k_{m123}, k_{b1}, k_{b3} and k_{b123}=constants which relate the local stresses to the rotations of concrete slab and of cross beam.

2.2 Structural Parameter for Concrete-Slab Rotation

Referring to Fig.4, the rotation θ_{s0} of concrete slab at the position (a, 0) where a main girder is located, is expressed by[3]

$$\theta_{s0} = (a/D_c)\{P/(2\pi^2)\}\varphi_p(x/a)\,\varphi(x/a)\Big[\sum_{m=1}^{\infty}\{(-1)^m/m^2\}\sin(m\pi x/a)$$
$$(1+m\pi|y|/a)\exp(-m\pi|y|/a)\Big] \tag{2}$$

where a=spacing between main girders, D_c=flexural rigidity of concrete slab, P=a concentrated load, $\varphi_p(x/a)$=correction factor for the wall parapets on both sides of the roadway, and $\varphi(x/a)$=correction factor to treat the concrete slab as a continuous plate.

Equation(2) implies that the concrete-slab rotation θ_{s0} varies with values of a/D_c. The values of a/D_c are determined by the dimensions of concrete slab. Hence the reciprocal of a/D_c, namely, D_c/a is chosen as a structural parameter for θ_{s0}. The bridges with smaller values for D_c/a are more susceptible to cracking, since the decrease of D_c/a increases θ_{s0} and then results in the

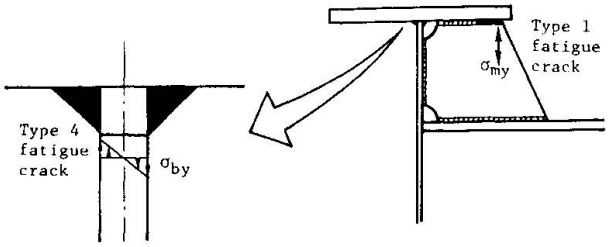

Fig.2 Local stresses σ_{my} and σ_{by}

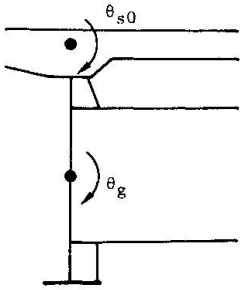

Fig.3 Rotations θ_{s0} and θ_g

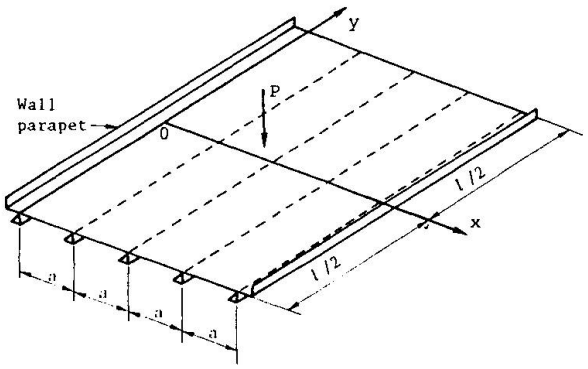

Fig.4 Concrete slab under concentrated load P

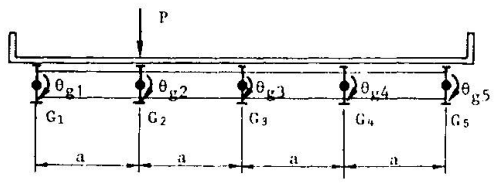

Fig.5 Cross-beam rotation θ_{gi}

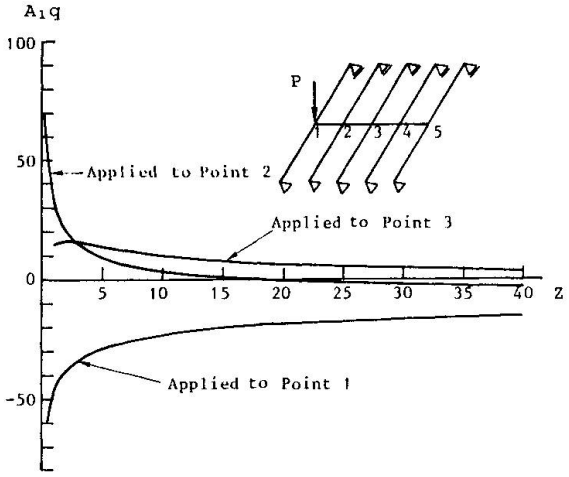

Fig.6 Relationship between $\mathbf{A}_1\mathbf{q}$ and z

increase of the local stresses of σ_{my} and σ_{by}.

2.3 Structural Parameters for Cross-Beam Rotation

In a plate girder bridge with five main girders as shown in Fig.5, the rotation θ_{gi} of the cross beam at the main girder G_i is given by[3]:

$$\theta_{gi} = \mathbf{A}_i\mathbf{v}/(56a) \tag{3}$$

where $\mathbf{v}=(v_1,v_2,v_3,v_4,v_5)^T$, v_i=vertical displacement of the girder G_i at the cross-beam connection, T=symbol representing transpose, and $\mathbf{A}_i$=row vector consisting of constants which correspond to θ_{gi}. When a concentrated load P is applied to the girder G_j, the vertical displacement v_i of the girder G_i is provided with

$$v_i = Pq_{ij}l^3/(48E_s r_i I_g) \tag{4}$$

where q_{ij}=load-distribution-coefficient from the girder G_j to G_i, l=span length of main girders, E_s=Young's modulus of steel, $r_i=I_{gi}/I_g$, I_{gi}=moment-of-inertia of the main girder G_i, and I_g=moment-of-inertia of any girder arbitrarily selected among the five main girders. The load-distribution-coefficient q_{ij} is expressed by a function of r_i and Z defined by

$$Z = (I_Q/I_g)\{l/(2a)\}^3 \tag{5}$$

where I_Q=moment-of-inertia of a cross beam. Substitution of Eq.(4) into Eq.(3) provides

$$\theta_{gi} = \{P/(2688E_s)\}\{l^3/(aI_g)\}\mathbf{A}_i\mathbf{q} \tag{6}$$

where $\mathbf{q}=(q_{1j}/r_1,q_{2j}/r_2,q_{3j}/r_3,q_{4j}/r_4,q_{5j}/r_5)^T$.

Figure 6 shows the relationship between $\mathbf{A}_1\mathbf{q}$ which corresponds to

the cross-beam rotation θ_{gl}, and Z. The calculation of $\mathbf{A_1 q}$ is carried out for all r_i=1. Except for the case of a concentrated load P applied to the girder G_3 above which a center divider exists on the roadway, $\mathbf{A_1 q}$ is approximately inversely-proportional to Z for Z≤10. Accordingly, when Z≤10, the term $\{l^3/(aI_g)\}\mathbf{A_1 q}$ in Eq.(6) is proportional to $\{l^3/(aI_g)\}/Z$, and then considering Eq.(5), $\{l^3/(aI_g)\}/Z$ is changed into $8a^2/I_Q$. On the other hand, when Z>10, only the term $l^3/(aI_g)$ is variable in Eq.(6), since $\mathbf{A_1 q}$ takes almost constant values for Z>10.

From the above, the following structural parameters are chosen for the cross-beam rotation θ_{gi}:

$$I_Q/a^2 \text{ for } Z\leq 10 \quad (7)$$
$$aI_g/l^3 \text{ for } Z>10 \quad (8)$$

The bridges with smaller values for these structural parameters suffer more chances of cracking, since the decrease of the parameters increases θ_g, which leads to the increase of the local stresses of σ_{my} and σ_{by}.

2.4 Relationship between Structural Parameters and Cracking

The relationship between I_Q/a^2 and initiation of Types 1 and 4 cracks is investigated for 158 plate girder bridges on a route of the Hanshin Expressway[4]. The structural parameter D_c/a is found to be almost invariable on this route.

Figure 7 shows the relationship between I_Q/a^2 and the number of bridges in which Type 1 cracks were detected. As shown in Ref.[4], the influence of θ_g on the local stress σ_{my} which causes Type 1 cracks is very small in the bridge with I_Q/a^2=3.1 cm^2. In Fig.7, however, Type 1 cracks occur in the bridges for I_Q/a^2>3.0 cm^2. This indicates that Type 1 cracks can be initiated by the

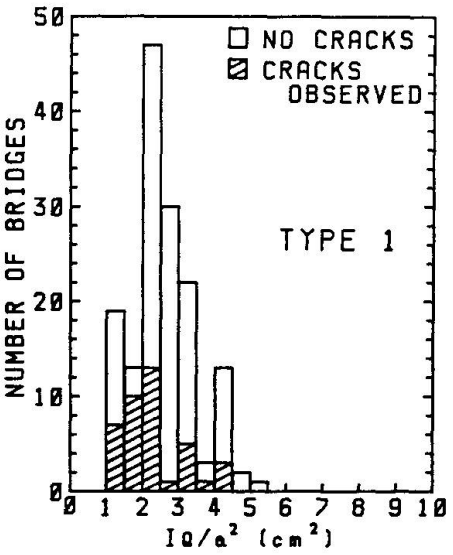

Fig.7 Relationship between I_Q/a^2 and the number of bridges in which Type 1 cracks were observed

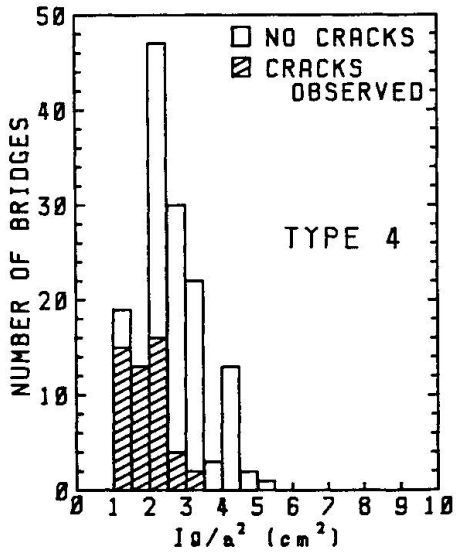

Fig.8 Relationship between I_Q/a^2 and the number of bridges in which Type 4 cracks were observed

concrete-slab rotation only.

Figure 8 shows the relationship between I_Q/a^2 and the number of bridges in which Type 4 cracks were observed. With the increase in I_Q/a^2, the number of bridges suffering from cracking gradually decreases, since the influence of θ_g on the local stress σ_{by} which causes Type 4 cracks becomes small. No cracks occur in the bridges for $I_Q/a^2>3.5$ cm^2.

3. FATIGUE TESTS OF CROSS-BEAM CONNECTIONS

3.1 Fatigue Test Specimens

As can be seen from Eq.(1), the local stresses σ_{my} and σ_{by} are provided with the sum of stress components due to the rotations of concrete slab and of cross beam. This implies that effects of concrete-slab rotation and of cross-beam rotation on the local stresses can be divided. Then in order to clarify the influence of the concrete-slab rotation on the cracking at cross-beam connections, fatigue tests are carried out on the specimens as shown in Fig.9. The specimens consist of cross-beam connections and of

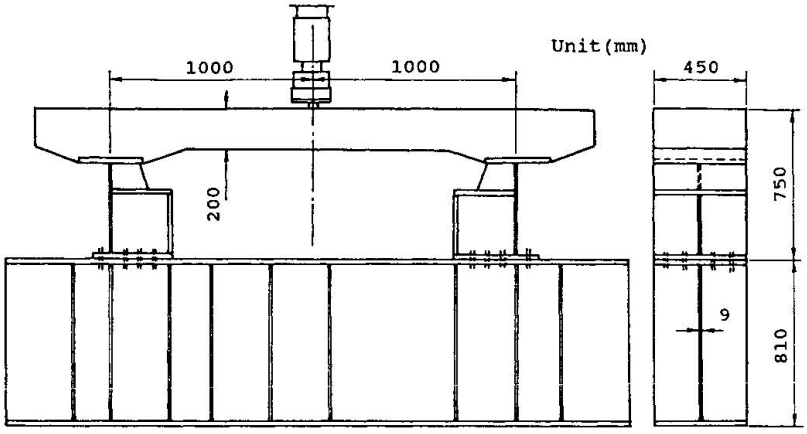

Series A

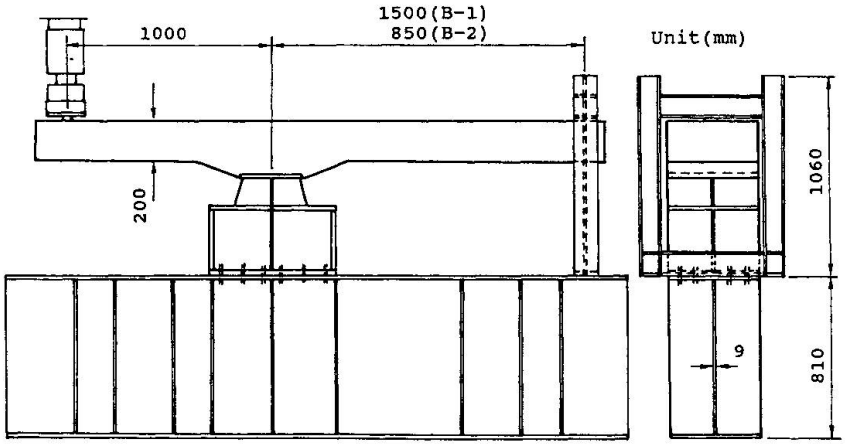

Series B

Fig.9 Fatigue test specimens

a concrete slab in a stripped form. The series A corresponds to the cross-beam connections of exterior main girders. The series B does for interior main girders. In the series B, negative moment is created in the concrete slab above the cross-beam connection.

3.2 Connection Details between Girder Flange and Concrete Slab

In order to examine the effects of connection details between girder flange and concrete slab on the cracking, the number of stud shear connectors and their arrangement are changed at each cross-beam connection, as shown in Fig.10. In the right side of Specimen A-2 and in Specimen B-2, a slab anchor is used.

3.3 Results of Fatigue Tests

The following observations are drawn from the fatigue tests:

-The similar cracks as shown in Fig.1 occur at all the cross-beam connections, not depending on the connection details between girder flange and concrete slab.
-In the series A corresponding to the cross-beam connections of exterior main girders, there exists no order in initiation of Types 1 and 4 cracks, while in the series B corresponding to the

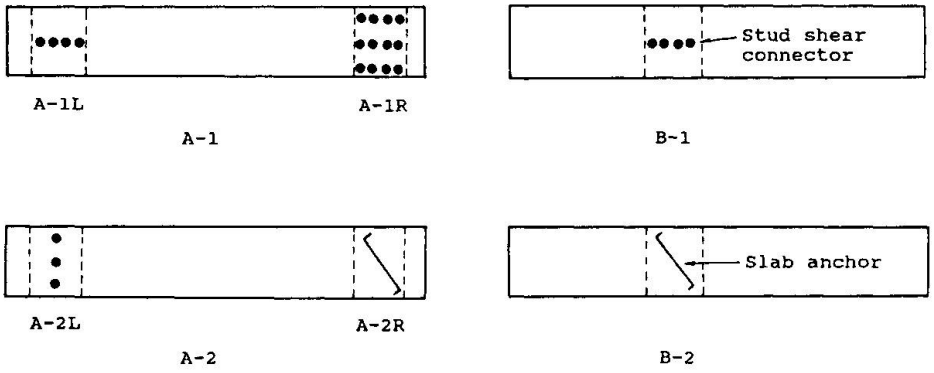

Fig.10 Connection details between girder flange and concrete slab

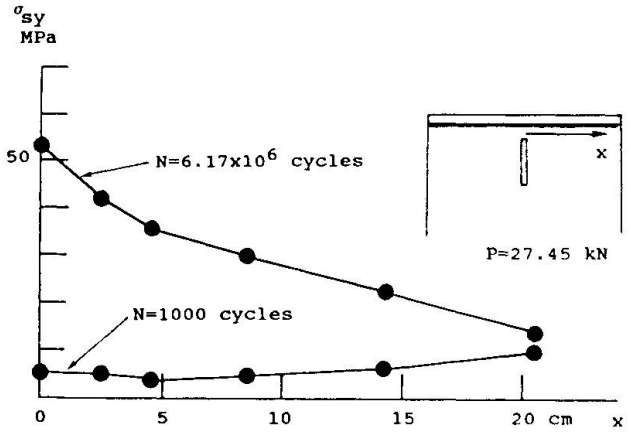

Fig.11 Distribution of web surface stress σ_{sy} along the flange-to-web fillet weld(Specimen B-1)

cross-beam connections of interior main girders, Type 4 crack follows Type 1 crack.

The distribution along the flange-to-web fillet welds of the stress σ_{sy} on the surface of the web plate is shown in Fig.11 for Specimen B-1. In the figure, at N=1000 cycles σ_{sy} is very small and Type 1 crack does not occur, while at N=6.17×10^6 cycles σ_{sy} becomes large and Type 1 crack is initiated and grows. Therefore in the series B the propagation of Type 1 crack makes the local stress σ_{by} increase, and then results in Type 4 crack initiation.

3.4 Characteristics of Occurrence of Local Stresses

In order to make clear the occurrence of the local stresses σ_{my} and σ_{by}, a finite element analysis is carried out for a model as shown in Fig.12. It consists of a girder flange, girder web and connection plate, and a half of them is divided into finite elements from symmetry. The bottom edges of the girder web and connection plate are fixed. The forces which are determined by the measurements of displacement of the concrete slab and by the measurements of strain of the stud shear connectors are applied to the girder flange of the F.E.M. model, as shown in Fig.13. The vertical forces on the girder flange are produced by the pull-out action of stud shear connectors and by the contact action between concrete slab and girder flange. The horizontal forces on the girder flange are created by the shear resistance of stud shear connectors.

Comparison of F.E.M. values with the measured ones is shown in Fig.14 for σ_{my} and σ_{by}. As for σ_{my}, F.E.M. values are close to the measured ones. As for σ_{by}, the distribution of F.E.M. values shows the same tendency as that of the measured ones, though the former shifts slightly from the latter.

The local stresses σ_{my} and σ_{by} can be correlated with the forces Q and S. Here Q is, as shown in Fig.13, the total of the vertical forces on the girder flange, while S is the total of the horizontal forces on the girder flange. The stress components of σ_{my} and σ_{by} against Q and S are listed in Table 1 for the series A. The stress values in the table are obtained at the points of the strain gauges nearest to the crack initiation in the fatigue tests. Connection A-0, which is just a model for the F.E.M. analysis, corresponds to the cross-beam connections in which neither stud shear connectors nor slab anchors are used between concrete slab and girder flange. In this model, the concentrated load of 49.0 kN is applied vertically to the edge of the girder flange just above the connection plate.

The following are pointed out from Table 1:

-The local stress σ_{my} is mostly produced by the vertical force Q, while the local stress σ_{by} is produced by both Q and S.
-The stress values of Connection A-0 are much smaller than those of any other connection model.

In order to reduce the local stresses and thus to prevent cracking, it is recommended that neither stud shear connectors nor slab

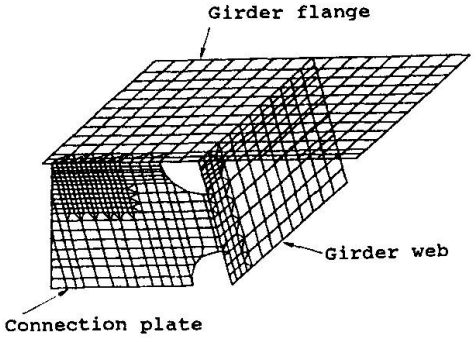

Fig.12 Mesh division

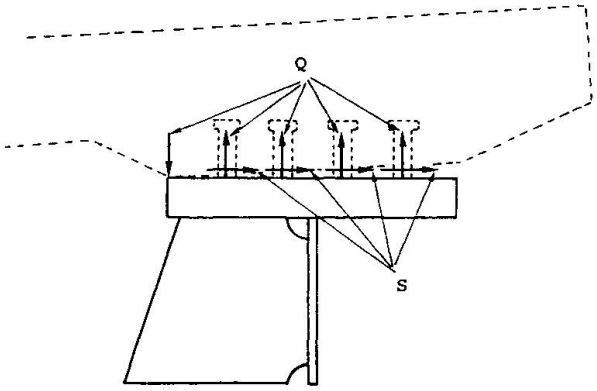

Fig.13 Forces acting on F.E.M. model

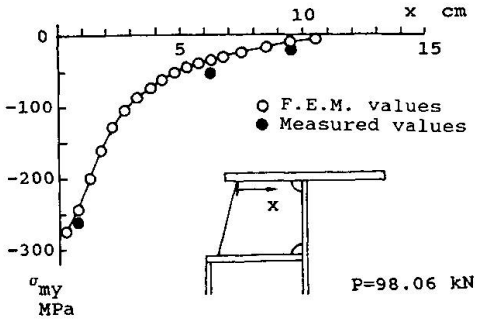

(a) σ_{my} at connection plate

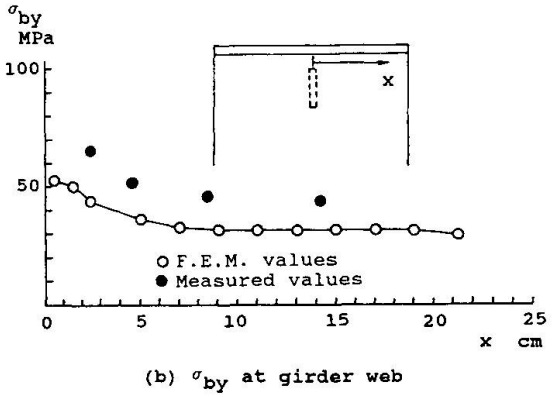

(b) σ_{by} at girder web

Fig.14 Comparison of F.E.M. values with measurement values(Connection A-1L)

Table 1 Comparison of stress components against Q and S

Connection	Q (kN)	S (kN)	σ_{my} (MPa)	σ_{mQ} (MPa)	σ_{mS} (MPa)	σ_{by} (MPa)	σ_{bQ} (MPa)	σ_{bS} (MPa)
A-1L	48.88	41.45	-237.9	-240.8	2.9	43.2	8.6	34.6
A-1R	49.17	56.43	-292.3	-296.2	3.9	96.3	49.2	47.1
A-2L	56.03	66.08	-275.4	-279.8	4.4	77.1	21.1	55.9
A-2R	42.02	44.32	-295.9	-298.9	2.9	26.5	-11.9	38.5
A-0	49.03	0.0	-184.0	-184.0	0.0	-9.7	-9.7	0.0

Note: $\sigma_{my} = \sigma_{mQ} + \sigma_{mS}$
$\sigma_{by} = \sigma_{bQ} + \sigma_{bS}$
σ_{mQ} = membrane stress component produced by Q
σ_{mS} = membrane stress component produced by S
σ_{bQ} = plate-bending stress component produced by Q
σ_{bS} = plate-bending stress component produced by S

anchors be placed above the connections of cross beams to main girders.

4. CONCLUSIONS

(1)The structural parameters governing the fatigue cracking at the connections of cross beams to main girders in plate girder highway bridges were specified as follows according to the rotations of

concrete slab and of cross beam:

a) For the concrete-slab rotation, D_c/a.
b) For the cross-beam rotation, I_Q/a^2 when $Z \leq 10$, and aI_g/l^3 when $Z > 10$. Here $Z=(I_Q/I_g)\{l/(2a)\}^3$.

The bridges with smaller values of the above structural parameters become more susceptible to cracking. Type 1 cracks at the connection plates can be initiated by the concrete-slab rotation only.

(2) From the fatigue tests to investigate the influence of the concrete-slab rotation on the cracking, it was revealed that cracks are initiated at the cross-beam connections with stud shear connectors regardless of the number of them and their arrangement, and that they are also initiated at the cross-beam connections with slab anchors.

(3) To reduce the local stresses and thus to prevent cracking, it was recommended from a F.E.M. analysis that neither stud shear connectors nor slab anchors be placed above the connections of cross beams to main girders.

ACKNOWLEDGMENT

The authors would like to thank Mr. H. Inoue, graduate student of Osaka University, and Mr. Y. Yamada, Takadakiko Co., Ltd. for their help in carrying out the fatigue tests. The first author would also like to acknowledge the Kajima Foundation, Japan, who offered him the traveling expenses for his presentation in EPFL, Switzerland.

REFERENCES

1. OKURA I., HIRANO H. and YUBISUI M., Stress Measurement at Cross Beam Connections of Plate Girder Bridges, Technol. Repts. Osaka Univ., Vol.37, No.1883, 1987, pp.151-160.

2. OKURA I. and FUKUMOTO Y., Fatigue of Cross Beam Connections in Steel Bridges, IABSE, 13th Congress, Helsinki, 1988, pp.741-746.

3. OKURA I., YUBISUI M., HIRANO H. and FUKUMOTO Y., Local Stresses at Cross Beam Connections of Plate Girder Bridges, Proc. of JSCE Struc. Eng./Earthq. Eng., Vol.5, No.1, 1988, pp.89s-97s.

4. OKURA I., TAKIGAWA H. and FUKUMOTO Y., Structural Parameters Governing Fatigue Cracking at Cross-Beam Connections in Plate Girder Highway Bridges, Technol. Repts. Osaka Univ., Vol.39, No.1980, 1989, pp.289-296.